

Manuscript Number: EPSL-D-18-01305R1

Title: Origins of the terrestrial Hf-Nd mantle array: evidence from a
combined geodynamical-geochemical approach

Article Type: Letters

Keywords: mantle convection; geodynamical modelling; mantle geochemistry;
crustal evolution; trace element partitioning

Corresponding Author: Dr. Rosemary E. Jones, MSc, PhD

Corresponding Author's Institution: University of Oxford

First Author: Rosemary E. Jones, MSc, PhD

Order of Authors: Rosemary E. Jones, MSc, PhD; Peter E van Keken; Erik H
Hauri; Jonathan M Tucker; Jeffrey Vervoort; Christopher J Ballentine

Abstract: The formation and segregation of oceanic and continental crust from the mantle, and its return to the mantle via subduction and/or delamination, leads to the development of distinct geochemical reservoirs in the terrestrial mantle. Fundamental questions remain regarding the location, nature, and residence time of these reservoirs, as well as the respective roles of oceanic and continental crust in the development of the mantle's geochemical endmembers. The Lu-Hf and Sm-Nd isotope systems behave similarly in magmatic systems and together form the terrestrial mantle Hf-Nd isotopic array. Here we combine a geodynamic model of mantle convection with isotope and trace element (TE) geochemistry to investigate the evolution of the Hf-Nd mantle array. This study examines the sensitivity to: TE partition coefficients used in the formation of oceanic crust; density contrasts between subducting oceanic crust and the mantle; and the formation and recycling of continental crust. We show that the fractionation between the parent (Lu and Sm) and daughter (Hf and Nd) species needs to be higher than is indicated by partition coefficients determined from the present-day melting environment. This is consistent with the suggestion of deeper mantle melting earlier in Earth history and an increased role for residual garnet. Subduction and accumulation of dense oceanic crust produces a large mass of incompatible TE enriched material in the deep mantle. This deep mantle enrichment appears to play a more significant role than the extraction and recycling of continental crust in developing the Hf and Nd isotope and TE compositions of the mid-ocean ridge mantle source. The corollary of this result is that the formation of the continental crust plays a secondary role, contrary to the currently accepted paradigm. Nevertheless, the inclusion of continental crust formation and recycling produces a broader model mantle array, which better reproduces the spread in the natural data set. This model also produces the Hf and Nd isotope and TE compositions of the upper mantle and continental crust, as well as deep mantle compositions similar to those of plume-fed ocean island basalts. Our model is consistent with continental growth models based on the Lu-Hf isotopic composition of zircon, which suggest that 50-70% of the present-

day mass of the continental crust is produced prior to 3 Ga, and that the recycling of continental crust becomes more prevalent after this time.

Department of Earth Sciences
University of Oxford
South Parks Road
Oxford
OX1 3AN
United Kingdom

13th March 2019

Dear Prof. Michael Bickle,

I would like to present our revised manuscript entitled '*Origins of the terrestrial Hf-Nd mantle array: evidence from a combined geodynamical-geochemical approach*' for consideration for publication in *Earth and Planetary Science Letters*.

I would like to apologise for this resubmission being late. Significant work was required to improve the explanation of our model methods and this took some time. In order to fully respond to the reviewers comments, and to clarify our model methods in the main manuscript, I am afraid we are now slightly over the word limit (6681). As stated previously, the number of references in our manuscript also currently exceeds the limit, but given the interdisciplinary nature of our study we found that including more references was necessary to give a full account of the relevant and current literature. The reviewers also suggested additional references, which have been added.

We hope that we have sufficiently answered all of the reviewers concerns by significant modifications to the manuscript and supplementary information. Thank you for your time and consideration.

Yours sincerely,

A handwritten signature in black ink, appearing to read 'Rosemary Jones', written in a cursive style.

Dr Rosemary Jones (corresponding author)

Department of Earth Sciences
University of Oxford
South Parks Road
Oxford
OX1 3AN
United Kingdom

1st October 2018

Dear Prof. Michael Bickle,

I would like to present the manuscript entitled '*Origins of the terrestrial Hf-Nd mantle array: evidence from a combined geodynamical-geochemical approach*', by Dr Rosemary Jones and co-authors, for consideration for publication in *Earth and Planetary Science Letters*.

Determining the physical process occurring in the deep Earth that account for geochemical compositions obtained from mantle-derived rocks, remains one of the outstanding challenges in Earth Sciences. One way towards a more robust understanding lies in combining geodynamical models, which obey physical laws such as the conservation of mass and momentum, with trace element partitioning and radiogenic ingrowth. In this manuscript we present the results of combining a geodynamical model of mantle convection with isotope and trace element geochemistry to investigate the geochemical evolution of the terrestrial mantle and crust, specifically the Hf-Nd isotope array. Due to the trace element partitioning behaviour, and the relative length of the parent half-lives, the Lu-Hf and Sm-Nd isotope systems are ideal for investigating mantle evolution and the growth and recycling of the continental crust. Our model results highlight that the deep recycling and storage of dense oceanic crust is fundamental in developing the isotopic and trace element composition of the depleted mantle, as well as the compositions of plume-fed ocean island basalts. In contrast to the currently accepted paradigm, the formation and recycling of continental crust plays a lesser role, however, the inclusion of continental crust formation and recycling in the model produces a better match to the global Hf-Nd data array. We consider our manuscript, combining chemical and physical processes and concerning the evolution of the Earth's interior, to fit ideally within the scope of EPSL.

The number of references in our manuscript currently exceeds the limit, but given the interdisciplinary nature of our study we found that including more references was necessary to give a full account of the relevant and current literature.

We should point out that one of the co-authors, Erik Hauri, sadly passed away on the 5th September 2018. Erik was instrumental in this work and had seen a recent version of the manuscript prior to his death. We hope that we can continue to keep him listed as a co-author.

Thank you for your time and consideration. If you require any further information please do not hesitate to contact me and we look forward to hearing from you in due course.

Yours sincerely,



Dr Rosemary Jones (corresponding author)

Response to reviewers for Ms. Ref. No.: EPSL-D-18-01305 (Origins of the terrestrial Hf-Nd mantle array: evidence from a combined geodynamical-geochemical approach)

Firstly, we thank the reviewers for their constructive comments on our manuscript. In this document our responses to the reviewer's comments appear in blue. In addition, our changes to the originally submitted manuscript are also shown in blue in the revised manuscript. We hope we have sufficiently answered any questions raised in this reply, and by significant modifications and clarifications in the manuscript.

Reviewer 1.

We owe Reviewer 1 and the Editor our apologies for not providing a clearer description of the geochemical modelling and in particular that of the treatment of melting. We have significantly clarified this in the revised Supplementary Information, including a worked numerical example, and added a shorter clarifying description to the main text. Our melt formulation is a rather simple parameterization of the formation of oceanic crust at mid-oceanic ridges by batch melting. Our approach is identical to that used in Christensen and Hofmann (1994) as further explored in Brandenburg and van Keken (2007) and Brandenburg et al. (2008). We follow their use of the terms 'eclogite' and 'harzburgite' which are not intended to be two separate lithologies but two components of a single peridotite lithology. For a well-mixed undifferentiated mantle, we have by design a 12.5% melt fraction that is similar to that required to form 7 km of MORB during decompression melting. Our formulation is not sensitive to changes in mantle temperature or volatile content but the use of separate eclogite and harzburgite tracers allows for a sensitivity to peridotite fertility.

1) Averaging the eclogite-harzburgite assemblage before melting may be problematic oversimplification. Melting an average source effectively limits the depletion in the mantle (harzburgite), and some of the information the geodynamical-geochemical model could provide gets lost (e.g., how the individual tracers for the different lithologies evolve). It could also be the main reason for the limited mantle depletion observed in all models shown up to Fig. 6.

As mentioned above, we treat the harzburgite and eclogite tracers as components of a single lithology. Averaging them together for the composition of the melting material simulates a single peridotite melting lithology (which is a good first order approximation for MORB). That the degree of melting increases with the number of eclogite tracers reflects not the fact of eclogite melting to a greater extent than harzburgite, but a more fertile peridotite (average) lithology that melts to a greater extent (at a given potential temperature, volatile content, etc.).

2) There must be a mistake in the formula for calculating the average concentration for the melting assemblage. Essentially you cannot add up concentrations, see my detailed comments below.

We failed to properly define 'concentration' in our submitted version. We have clarified that we are summing the number of atoms, and updated the notation in the equations to help clarify our algorithm (which closely follows that of Christensen and Hofmann, 1994). α_{total} is the bulk composition of the melting zone (rather than the average composition); the average composition C_0 is α_{total} divided by the mass of tracers in the melting region. We distribute the atoms in a mass-conservative manner between the basalt and eclogite tracers that are in the melting zone as described in our updated supplementary material and demonstrated in the worked example.

3) After melting an average eclogite-harzburgite assemblage, which does not account for different melting and partitioning behavior of the lithologies, the redistribution between eclogite and harzburgite is non-trivial. It maybe my ignorance, but I cannot make sense of what is done in the 4th formula in the Appendix.

We have revised the supplement to clarify this important issue. Our approach is to redistribute the number of atoms present in a melt zone to the melt (eclogite tracers) and residue (harzburgite tracers) using batch melting equations that depend on melt fraction and partition coefficient. We have also provided a worked example for a single melting event for a single isotope system to show how our algorithm works.

4) The apparent sensitivity to the D values probably results from a combination of factors in the simplified melt model, rather to an actual problem with the D values. Other than the D value, the degree of melting (F) is a key parameter for melting models, and the way F is defined (as a function the relative abundance of eclogite and harzburgite tracers) leads to a severe underestimation of the degree of melting for realistic eclogite/harzburgite ratios (see my detailed comments to the supplement) . In any case, the resulting melt concentration is a function of D and F, and the way melting is done (batch vs. fractional), but the way F is defined may cause effects that may falsely be attributed to problems with the D values. The combined effects of melting an average assemblage with average D, and F that scales with the proportion of eclogite and harzburgite tracers, and subsequent redistribution between the different tracers may cause many effects that are (falsely?) attributed to just one parameter: D.

We agree with the reviewer that the simplified algorithm for batch melting introduces a resonance between melt fraction (f) and partition coefficients (D) such that one cannot use the modelled partition coefficients as 'true' partition coefficient. Where necessary, we have clarified this in the manuscript (e.g., lines 293-295). However, it should be noted that the partition coefficients we have implemented in our preferred model are still within the range of published partition coefficients for the different elements, as given in Table 1. In addition to this we have also run an additional model where we increase the melt fraction in the model by 25% and we show that the model results (average esp Hf and eps Nd and TE composition of the upper mantle) is relatively insensitive to melt fraction. This additional model information is shown in supplementary Figure S9 and Table 3 (see line 330).

Overall, the way melting is done, including the many simplifications and dependencies of parameters, makes it difficult to track the sensitivity to the different parameters. A simpler way to do the melting would be to use a mass flux for each element and tracer, i.e., eclogite and harzburgite. Such a mass flux combines the melting style and D-F into a single parameter that is easy to track. Plus, the mass flux can be done individually for each lithology and thus no averaging and redistribution is necessary (whose effects on the model are difficult to evaluate and may interfere with other parameters). The rationale behind is that for partial melting of peridotite beneath ridges with F of ca. 5-10% and Ds as given by experimental studies (your table 1), 84-98% of the Nd go into the melt, and 60-85% of the Sm and Hf, and about 20-40% of the Lu. So almost all the Nd, but also most of the Sm, Hf go into the melt, but less of the Lu. Mafic lithologies (eclogites) melt to a much higher extent than peridotites, i.e., that effectively all of the Sm-Nd-Hf and Lu go into the melt. Hence my recommendation would be to use "retention" factors similar to what is done for modeling formation of the continental crust. These retention factors (or mass of element transferred from source to melt) can be related to D and F with simple models and scaled appropriately for the

different elements for peridotite, and would effectively 0 for mafic lithologies (owing to the high expected F).

We hope our clarification that we use the eclogite and harzburgite tracers as two components of a single lithology is sufficient, along with the explicit acknowledgment of the resonance between f and D is sufficient here. We are certainly aware that our simple batch melting approach is only a first-order approximation to actual melting effects at mid-oceanic ridges and we hope to include more intelligent approaches in the near future (as much as we hope to be able to provide a quantitative understanding of the extraction/retention coefficients for continental crust extraction by explicitly taking into account the differentiation processes at subduction zones).

This approach would also allow directly tracing the concentration of each tracer individually, which would avoid potential artifacts from melting average assemblages and redistribution after melting. Please see our response to points #2 and #3 above.

Overall my recommendation for revising the paper is to better explain how melting is done, in the main text, and clarify some of the (potential) issues mentioned in my comments. This would be the minimum effort necessary. The article would also benefit a lot from making the writing more succinct. Often the text is very wordy, with unnecessarily complicated sentence structures, especially in the introductory chapter. I have made some suggestions for improvement in the detailed comments, but there are many more instances where text editing would be beneficial.

However, my preferred way for revision would be to modify how melting is implemented in the model, using simple element(mass) fluxes for the two lithologies. Different scenarios can then be investigated for different mass fluxes, and the compositions of each tracer be followed individually. Because the mass fluxes relate to D , F and style of melting, realistic bounds for these mass fluxes can be set with simple fractional melting models for realistic F and D values. The compositional variability can then be related to a single parameter, the element mass fluxes, and this would make the model much more transparent, and less prone to having a combination of effects that are then traced back (maybe falsely so) to only a single parameter (D).

We again hope that the clarification of the melt algorithm is satisfactory in this regard. We thank the reviewer for the numerous suggestions to improve the writing.

Detailed comments

line 38-39: to avoid misunderstanding rephrase: "the formation of oceanic crust at spreading ridges and continental crust through arc volcanism ..." [Completed](#)

line 59-62: simplify: "OIBs have a wide range of isotopic compositions, which have been grouped into different categories (e.g., EMI, EMII, and HIMU; White, 1985; Zindler and Hart, 1986; Stracke et al., 2005)" [Completed](#)

line 65: lower continental crust (Willbold and Stracke, 2006; 2010) [Completed](#)

line 67: add reference to Zindler and Hart, 1986, and add e.g., before these references because there would be many more to be cited. [Completed](#)

line 69: simplify: "...are related to recycled oceanic crust..." [Completed](#)

line 72-73: HIMU OIB...enriched in U due to interaction with U-rich continental sediments (Elliott et al., 1999). Really? I do not think this is quite what Elliott et al. (1999) are saying. It is true that Elliott et al. 1999 don't make the explicit link between recycling of U enriched oceanic crust and the development of the HIMU mantle endmember, but they do state in their conclusions that 'After the dramatic increase in oxygen fugacity of the atmosphere at the end of the Archean, U can be readily weathered from the continents in its highly soluble, oxidised state. Alteration of the oceanic crust incorporates U delivered from the continents to the sea, and recycles it into the mantle preferentially relative to insoluble Th. The flux of recycled U necessary to appropriately lower upper mantle Th/U is within the bounds obtained by integrating present day fluxes of subducted 'excess' U for ~2 Ga.' Other references go on to link this with the HIMU mantle endmember. We have added the reference of Hanyu et al. 2014 to address this and have specified in the text that this is suggested to have occurred after ~2 Ga.

line 73-74: "In contrast to the OIB source region, the source of mid-ocean ridge basalts (i.e., the upper mantle) is more homogeneous in composition (Hofmann, 1997)". This statement is not true, see Hofmann (2014, Treatise Geochemistry) and recent MORB compilations (e.g., by Gale et al., 2013). We have removed this. The section now reads – 'The source of mid-ocean ridge basalts (MORB) is referred to as the depleted MORB mantle (DMM) reflecting its chemical depletion in incompatible TE as a result of upper mantle melting and the formation of oceanic crust.'

line 75: I would simply call it depleted mantle (DM). We have changed this to the depleted MORB mantle as this is what it is referred to through the rest of the manuscript.

line 77: "The study of the geochemical evolution of the Earth can be augmented by mass balance modeling." Weird statement, rephrase. Rephrased to 'Mass balance modelling is a useful way to investigate the geochemical evolution of the Earth.'

line 80: add reference to Kumari et al., 2016 Completed

line 102: well-stirred, not well-mixed Completed

line 109-112: lengthy explanation of epsilon notation for Nd and Hf can be omitted. Given the interdisciplinary nature of our paper we felt it would be useful to the reader (particularly the non-isotope geochemist) to define what is meant by epsilon values and CHUR, as they are referred to extensively throughout the paper. On this basis we still feel that it is important to include this information, but the journal could perhaps put it as a footnote if it is not considered necessary in the text – we will suggest this at the editing stage.

line 114-115: the region cannot be negative or positive, only the Eps values, use more exact wording Changed to 'In this array the DMM shows positive ϵ_{Hf} and ϵ_{Nd} values and enriched mantle compositions (EMI, EMII) extend to negative ϵ_{Hf} and ϵ_{Nd} compositions.'

line 119: closely follow or use the same approach? If there are differences, mention briefly what they are in the main text. Completed.

The next series of comments and questions (through to the one for lines 149-151) are, we hope, addressed sufficiently in the main points above. We have clarified the main text where necessary and significantly improved the explanation of the model methods in the supplementary information.

line 128-135: I am confused by the terminology here, and in the end, I do not understand how melting works in the model. You need to have same ultramafic mantle that melts, including any recycled oceanic crust, and you need to distribute both "tracers (mafic and ultramafic) between melt and residue. However, in line 128 oceanic crust = eclogite, in line 131-132 it is stated that: any tracer that melts to form oceanic crust = 'eclogite'. The statement in line 135 seems to suggest that you form oceanic crust simply by melting former recycled oceanic crust? But what melts to form oceanic crust is mantle (peridotite) plus recycled mafic crust (eclogite). The supplement sheds more light on some of these issues, but I also have some issues with the way melting is done, see my comments below.

line 141-143: delete the statement reg. noble gases, off the point here. [Completed](#)

line 144: what do you mean by "melting events are accumulated in 5 Myr intervals". Is it that all melt generated in 5Ma is accumulated and then forms a new "eclogite" tracer? Again, the supplement sheds more light on this, and some of the explanation given there should go into the main text. See my comments to how this queuing up of tracers, i.e. how many of them accumulate before melting, should have an influence on the variability created in the model.

line 145: "concentrations are evenly distributed over all the tracers that have accumulated in a melting zone". Again there should be mafic and ultramafic tracers in the melting zone, and these should have different concentrations. So if both mafic and ultramafic tracers have the same concentrations this would be an oversimplification that needs some justification.

line 146: batch melting equations are easy to use, but so are fractional melting equations, which come closer to the natural process (e.g., Kelemen et al., 1997), what is the degree of melting? Does it vary or is it a fixed value? Again supplement gives some explanation, but the way F is defined seems problematic, see other comments.

line 149-151: "...this study limits the partition coefficients used to those derived from natural samples (e.g., Kelemen et al., 2003; Salters and Stracke, 2004; Workman and Hart, 2005) and not those that have been derived experimentally ..." this statement is incorrect. The cited studies use experimentally determined D values for their calculations of bulk D . Rephrase.

line 165: add reference to Kumari et al., 2016 [Completed](#)

line 171: it is true that the oldest crust is about 4Ga, but the non-chondritic initial isotope ratios (e.g., for Nd and Hf) in these rocks indicate that silicate differentiation must have started much earlier, which is consistent with the ^{142}Nd isotope systematics in Archean rocks. Thus, producing crust started earlier, perhaps as early as 4.56Ga.

[According to Jeff Vervoort's work \(currently in prep.\) Hf isotope compositions of zircons, with reliable age determinations, suggest there is no significant depletion of the mantle reservoir before 3.8 Ga. On this basis they suggest that there can be little significant continental crust formation prior to this time. We agree that the comment about \$^{142}\text{Nd}\$, but it is not clear how this relates to the long term record of continental crust formation. On this basis, we believe our selection of a starting age of CC formation of 4 Ga is appropriate for this model. We also show the result of delayed mantle depletion, starting at 3.8 Ga, in the supplement \(Figure S8\), to give the reader some indication of the model sensitivity to this.](#)

line 177: how does the "redistribution" work? Do you mix with other tracers and get one new homogeneous isotope ratio, or do you preserve the crustal isotope ratios and have different "eclogite" tracers with different isotope ratios, that are somehow (statistically) distribute in the mantle? Please see our response to the main points above. The chemistry is dealt with as number of atoms of each isotope species of interest. Isotope ratios are then calculated on this basis. To improve clarity this section has been reworded to – ‘When this functionality is applied, a fraction of the number of atoms of each isotope species (e.g., ^{176}Lu , ^{176}Hf , ^{177}Hf , ^{147}Sm , ^{143}Nd , ^{144}Nd), contained in the continental crust at a particular time interval, are removed and evenly distributed to the eclogite tracers that have just participated in a melting event (i.e., the newly formed oceanic crust).’ Additional information and a worked example can be found in the supplementary information.

line 185-186: the continental crust composition based on the loess estimate of Chauvel et al. (2014) is problematic, as it is hardly representative and probably the eps Nd is too high. See the compilation of global shales from Dhuime et al. (2017), which has a present-day average epsNd of -17.8 (range from 0 to -44), based on a much larger number of data (global shales). We are afraid that we were unable to find the epsNd value suggested here in the cited paper. As such we contacted the author. Bruno Dhuime said the running epsNd median of his data compilation from shales is about -10 at present, which is similar to the estimate based on loess made by Catherine Chauvel et al. He wasn't sure where the -17.8 value came from, so at this time we will stick to using the CC composition of Chauvel et al. (2014). In addition, we have added some clarification on the eps Hf and esp Nd compositions generated for the continental crust in the model in response to a comment from reviewer 2 (see lines 443 – 446).

section 3.2: in your melting scenario, D and F are the variables. You discuss variability in D in detail, but what is the (range of?) F applied? Again, the supplement gives some information, but see the other comments. F has even similar or greater influence than D. Note that bulk D values also change during progressive melting. In your case this is relevant for melting across the garnet-spinel transition. Melting at ridges (often) starts in the garnet stability field, but most melting is done in the spinel field. So neither the D for spinel field melting (e.g. 2GPa of Salters) or garnet melting (e.g. 3GPa of Salters) alone will be appropriate. See my general comments, use "retention coefficients" for mantle melting as well (similar to what you do for the CC). Please refer to the responses to main points above. In addition, and as suggested in the responses to the main points above, we are not suggesting the bulk D values implemented in our preferred model are the true values and we have highlighted this in the revised manuscript (lines 293-295). Essentially, we are treating the bulk D values as a variable in the model. Although, the bulk D values we implement are within the range of published bulk D values, as given in Table 1, and therefore we do not consider the values to be completely arbitrary. We also suggest that the adjusted bulk D values do consider some of the subtleties that the reviewer refers to above. For example, we suggest that in order to sufficiently fractionate the parent from daughter species in order to generate the observed isotopic compositions that melting must occur in the garnet stability field for at least part of Earth's evolution.

line 283-284: "The models presented thus far fail to produce the observed radiogenic Hf and Nd isotope composition of the upper mantle". If you are always mixing all tracers to have a homogeneous isotope composition before melting (as implied by the statement in line 145, see

comment above), this would be no surprise, because this mixing effectively keeps the mantle (harzburgite) from becoming progressively depleted. [Please see response to main points above.](#)

line 297: delete statement. [Completed](#)

line 299: "...higher BSE starting compositions of Palme and O'Neill (2003)..." higher than...what? Reworded to 'For example, the BSE concentrations of Palme and O'Neill (2003) are higher for Lu, Hf, Sm and Nd compared to McDonough and Sun (1995). When these concentrations are utilised this also results in a more TE-enriched upper mantle and, in this case, the composition of a MORB with 9 wt.% MgO can be matched with a higher melt fraction (Table 3).'

line 302: the melt fraction for MORB is (too) high compared to typical estimates, which range somewhere between 5 and 10%.

There was an error presented in Table 3, with the wrong values underlined as being the best match to a MORB composition with 9 wt.% MgO. The expected concentrations (as presented in supplementary figure S4) are 1.33 ppm for Hf and 5.5 ppm for Nd. The correct values (i.e., the best matches) have now been underlined in Table 3 and this corresponds to a melt fraction of around 10% to 15% - the upper limit of what is suggested by this reviewer, and what is suggested to be an appropriate F value by reviewer 2.

line 307: I think I know what you want to state here, but perhaps rephrase anyway. We have no access to such lower mantle materials so how would we measure them? Reworded to – 'Specifically, the values observed in the lower mantle spread to compositions not measured in OIB samples that are thought to be sourced from the lower mantle (Fig. S7).'

line 343-345: same comments as in line 149-151, also what about different extents of melting? In line with the revisions made above this line has also been reworded to – 'Overall the model suggests that elemental partition coefficients, combined with present-day mineral abundances and melt fractions, may not be appropriate for the entire of Earth evolution.'

line 375: also reference Willbold and Stracke, 2006; 2010 [Completed](#)

line 388: but you do have a mass flux from the CC into the mantle, i.e., you do recycle part of the CC into the mantle (simply your model does not tell if it is via subduction of sediments or delamination, etc.). Provide more explanation. We do recycle CC into the mantle in our final preferred model, but the vast amount of the Hf-Nd isotopic array can be produced by the recycling of oceanic crust alone – as indicated by the figure (S5) referred to, which doesn't involve the formation or recycling of CC. The reason for suggesting that the recycling of oceanic sediments might be required to explain the full Hf-Nd isotope array is that oceanic sediments themselves have a shallower Hf-Nd array and therefore if mixed into the mantle could generate the extreme HIMU and EMII compositions. We have reworded this section to improve clarity – 'In contrast, our model results show that a large proportion of the Hf-Nd mantle array can be produced by the recycling of oceanic crust alone (Fig. S5). Producing and recycling CC produces a wider spread in the Hf-Nd isotope array (Fig. 7), but recycling oceanic sediments into the mantle, which have a shallower Hf-Nd isotope array (Chauvel et al., 2008) (not modelled here), may be required to generate the full array (i.e., HIMU and extreme EMII compositions).'

line 408-411: again this might simply be an effect of "mixing all tracers to have a homogeneous isotope composition before melting" (statement in line 145), because enriching the harzburgite by mixing in eclogite makes the entire assemblage less sensitive to mixing in of enriched CC material. [Please see response to main points above.](#)

line 413-416: you also have to consider that the CC is significantly more enriched in the incompatible elements than the oceanic crust. There is about a factor of ten less mass of the CC than oceanic crust, but Lu-Sm-Hf and Nd have 5-14-18 and 28 times higher concentrations in the CC, so about the same mass of element in the CC and oceanic crust. But if you limit the flux from CC into the mantle, but all oceanic crust goes back and gets remixed, then oceanic crust may have a bigger effect.

[We agree with the reviewer here about the relative enrichment of the incompatible TE in the continental crust and therefore you might expect about the same mass of an element in the CC as the OC, and therefore for them to have similar effects. However, we do not agree that OC recycling is responsible for mantle depletion, rather the storing of a large mass of OC at the CMB when an increased eclogite density is applied \(e.g., as highlighted in lines 26-30\). When no EED is applied to the OC the recycling is efficient \(i.e., the mantle is well stirred in the model\) and any heterogeneity caused by mantle melting to form OC is erased \(as shown in Figure 5 a and d\). The reason that OC has such a big effect on the mantle depletion in the models presented here is because the majority of it \(particularly in the high EED cases\) tends to accumulate at the CMB and is effectively sequestered from the convecting mantle. The modelling shows that these deep pools are as good, if not better, repository to sequester incompatible trace elements as the CC. We have added some additional lines to the discussion to clarify this point \(e.g., lines 422-423, 426-429 and 476-478\).](#)

line 422: over-deplete? rephrase, because we essentially do not know what the limit of mantle depletion really is, see your discussion in lines 347-359. [For clarity we have removed this sentence.](#)

Supplement: Geochemical modeling

binning by 5My time intervals: this should be a parameter that determines the number of tracers (n) involved in melting event, which in turn should influence the overall variability generated by melting, which should scale with \sqrt{n} . So how many tracers are in the melting region, and how does the variability change if this number is changed? Would be helpful to discuss this briefly. [We have addressed this in the supplementary information](#)

There must a mistake in the first formula, you cannot add up concentrations, they have to be multiplied by the mass and then the total concentration divided by the total mass of the system:

$$C(s) = [\sum(C_i(s) * n_i) + \sum(C_j(s) * m_j)] / (\sum(n_i) + \sum(m_j)), \text{ n and m being masses}$$

when you then melt the average eclogite-harzburgite assemblage, with a common D and F you ignore that different lithologies have different Ds and melt to quite different extent for the same mantle temperature due to their different solidii.

So this is a simplification, but it leads to lower degrees of melting for the eclogite and higher degrees of melting for the peridotite compared to what would actually be expected and the partitioning may also differ.

Furthermore, you define $f=N/(N+7M)$, so essentially you are asserting that the amount of melt generated is equal to the amount of eclogite tracers in the system. This makes some conceptual sense in context of the model, but not when it comes to actual mantle melting, as F depends on the ratio of N/M , which typically should be no more than $1/10$. In this case f would be ca. 1.5%, which is way too low for melting underneath ridges (ca. 5-10%). To get to realistic F you need $N/M < 1/2$, which is way too high.

As stated F is calculated depending on the proportion of eclogite to harzburgite tracers present the melt zone and using the equation $f=N/(N+7M)$. The model has an equal number of eclogite and harzburgite tracers, hence the multiplication of M (harzburgite tracers) by 7. This means if there are an equal number of eclogite and harzburgite tracers then $F=12.5\%$. This is slightly higher than melt fractions suggested by this reviewer of between 5 and 10%, but we consider it a reasonable melt fraction for melting at MOR (also supported by reviewer 2). If there are half the number of eclogite tracers than harzburgite (likely when some of the eclogite tracers are being stored at the CMB when excess eclogite density is applied) then $F=6\%$. We have added some additional information on this to the supplementary material, and we have included a sentence on how F is calculated in the manuscript methods section (see lines 148-156).

I can also not make sense of the redistribution of the total residue concentration (Cr) between the eclogite (Ci) and harzburgite (Cj). This seems a non-trivial problem as the concentration of the eclogite-harzburgite assemblage was averaged before melting, this average melted, leaving behind an average residue (Cr).

My point is, you need to treat melting of the lithologies individually, otherwise you run into trouble.

See my general comments for a way out.

[Please see response to main points above.](#)

Reviewer #2:

My understanding of what is described is that the authors did a simple batch melting calculation (fair enough given the uncertainties) but I could not find the value chosen for the melting degree (1%, 10%, 20%?). ([see responses to Reviewer 1 comments on F](#)) They also create confusion because they list a range of potential source mineralogies (see bottom of Table 1) but do not necessarily explain what was used to calculate a given model. For example:

(a) Was the mineralogy listed for 'simple peridotite' ever used to calculate D values? If yes, where are the values listed and are they plotted somewhere?

[Simple peridotite is not used to calculate any \$D\$ values and has been removed from Table 1.](#)

(b) Which mineralogy was used to calculate the model plotted in figure 3e? Is this mineralogy listed in one Table, and did this mineralogy include residual garnet? This key element is not given.

[It is the mineralogy for Salters and Stracke \(2004\) - 2 GPa – DMM that has been used to calculate Fig 3e \(i.e., without garnet\). We have updated the figure caption and text on the figure to clarify this.](#)

I doubt that the detailed differences between mineralogies have much impact of the final results; the only important factor is the presence or absence of garnet in the source and the residual solid. I therefore recommend that the authors use only two mineralogies: one without garnet and one with garnet. This will make the model simpler to understand for the reader.

Showing the full variation in the range of bulk D values that can be calculated depending on the selected mineral/melt partition coefficients (K_d) and mineral modes (as shown in Table 1) is important for later reasoning when we test the sensitivity of the model to the full range of possible bulk D values from published values. We agree that the presence or absence of garnet has a big effect (as Lu is shown to be compatible in garnet), but the point of Figure 3 is to show that the model is highly sensitive to the choice of partition coefficients regardless of whether garnet is involved or not. In light of the reviewers comments we have tried to simplify Table 1 (including relating the bulk D values to the specific figures) and to specify exactly in the text which partition coefficients are being used when.

It is also clear to all geochemists that the slope of the Nd-Hf isotopic array is controlled by two main factors if its existence is attributed to melting alone: the ratio of $(D_{Lu}/D_{Hf})/(D_{Sm}/D_{Nd})$ during the melting event, and the age of the fractionation event. The authors make a clear statement about the impact of the fractionation age and use a color coding to show it in several figures. They are far less clear about what control the $(D_{Lu}/D_{Hf})/(D_{Sm}/D_{Nd})$ ratio and they do not express unambiguously that their best model involves melting with residual garnet (I suspect so since the K_D value of Lu is very high!!). Since they also do not provide the percent melting used in the calculations, it is impossible to evaluate if the model is petrologically reasonable.

We have now also provided clarification about the melt fraction used in the model (see lines 148-156) and we do provide detail in the discussion about the potential increased role for garnet in the melt source region. However, we accept that there is unlikely to be significant garnet in the present-day MORB source but think this may have been the case in the geological past (i.e., when the mantle was hotter and melting occurred deeper). We have added some additional discussion and supporting references for this (lines 337-355). In addition, as highlighted in response to comments from reviewer 1, the bulk D values that we implement should not be taken as the actual values (lines 293-295), but rather they demonstrate that in order to produce the isotopic composition of the upper mantle we need to increase the relative fractionation of the parent (Lu) and daughter (Hf) isotope species during mantle melting, and one way of explaining why this, which has been suggested before to explain the Lu-Hf, Sm-Nd isotope systematics and HREE patterns of MORB (e.g., Salters and Hart (1989) and Hirschmann and Stolper (1996)), would happen is to invoke the presence of garnet in the melt source region.

The end result is that Lu must have a high K_D value for the model to fit the slope of the Nd-Hf mantle array. This requires the presence of a significant amount of residual garnet when MORB is produced. Given the known trace element pattern of MORB, the absence of HREE fractionation in MORB and the abundant literature on the subject, this interpretation does not look very realistic. In addition, the argument of higher residual garnet in the earliest part of Earth history does not really hold when looking at the trace element pattern of Archean mafic lavas (komatiites and basalts) that never show any sign of residual garnet.

The reviewer is correct that in order to obtain the naturally occurring Lu-Hf compositions, we need to have some garnet present in the melt source region. However, as the bulk D values we present should not be taken as actual bulk D values (as highlighted in lines 293-295) we cannot calculate exactly how much residual garnet would be required. But we envisage, due to the high K_D of Lu in garnet, that the presence of even a small amount of garnet in the melt source region would result in a lower amount of Lu relative to Hf being partitioned into the oceanic crust and could account for the Lu-Hf and Sm-Nd isotope systematics of the mantle.

We are not the first to suggest that garnet in the melt source region helps to explain the ϵ_{Hf} and ϵ_{Nd} of MORB. Salters and Hart (1989) state ‘A sequential melting model, in which melting starts in the garnet stability field and then continues at shallower levels, best explains the combined Nd and Hf isotope systematics, and is compatible with our present geophysical and geochemical knowledge of mid-ocean-ridge magmatism’, although a criticism of this paper is that melting at this depth would produce more than the ~7 km thickness of oceanic crust observed. However, this could have been the case in the early Earth when the produced crust is thought to have been thicker. Hirschmann and Stolper (1996) suggest that the Lu/Hf-Sm/Nd systematics of most MORB can be accounted for by melting of a spinel peridotite/garnet pyroxenite mantle provided that the source region contains 3–6% pyroxenite with $\geq 20\%$ modal garnet. This again, agrees with the results we find from the combined geodynamical-geochemical modelling. We have included these additional references in the discussion (lines 337-355).

One result of a higher melt fraction in the early Earth is that it may lead to a flatter REE pattern. A recent paper by Keller and Schoene (2018) even argued that there might not be any residual garnet because all the garnet (and CPX) could have been exhausted due to the higher degrees of melting. In terms of komatiites, there are some that show depletions in HREE that would suggest residual garnet and numerous studies have advocated that certain komatiites (Al-depleted) derive involve residual or fractionated garnet (e.g., Takahashi 1990, Gruau et al., 1990, Schneider et al., 2019 and references therein). As for the Archean basalts we suggest it is not certain what these basalts represent, for example, they could be continental and therefore not representative of Archean MORB. Due to uncertainties related to origin we have decided not to include a discussion of Archean basalts and komatiites in this manuscript.

I encourage the authors to look at alternative models: create MORB in usual conditions (about 10% melting in the spinel peridotite field), acknowledge that the formation and recycling of oceanic crust alone does not reproduce the Hf-Nd mantle array, and then try to constrain the necessary fractionation during continental crust formation (with or without crust recycling). Such model would be drastically more convincing. It would also have the advantage to recognize that continental crust formation depletes the mantle over Earth history, a feature that is not questioned by the scientific community.

We believe that we do carry out what the reviewer suggests here, and we hope that this is now clearer with our improved explanation of what melt fraction we are using (12.5%, lines 148-156). In the models presented first (shown in figures 3, 4 and 5) we use different published bulk D values, such as Salters and Stracke (2004) for 2 GPa (i.e., in the spinel peridotite field), to generate oceanic crust in the model and this is recycled and stored to a different degree in the lower mantle depending on the excess density implemented. Although the spread in mantle compositions don’t do a bad job of matching the Hf-Nd mantle array (see Figure 3e), they do not match the ϵ_{Hf} , ϵ_{Nd} , and trace element compositions of the upper mantle (e.g., as outlined in lines 239-241). We then go on to produce CC and recycle continental crust in the model and we still don’t see a match to the upper mantle compositions (lines 277-281), so we need to do something else to increase the depletion of the daughter species in the upper mantle, and as explained (lines 283-291) the only satisfactory way we have found to do this is to increase the relative fractionation of the parent and daughter species during mantle melting and to store recycled oceanic crust in the lower mantle. This could be accounted for by an increased role for garnet in the melt source region in the early Earth. We have added some additional explanation in the manuscript to clarify our approach.

More detailed comments:

Table 1 and Table 3 present the key parameters used in the various models but what is listed is not very clear. Table 1 is in fact a mixture of two independent tables. The first one (columns Ref to Garnet) reports the KD values published by other authors: it could be provided in a supplementary file. I am not sure that the selected set of KD values is the best but it is not important because using other values would not really change the big picture. The rest of the table (column Mineral Mode to (DLu/DHf)/(DSm/DNd) should in fact be linked to the bottom part of the table (Simple peridotite to Garnet). As mentioned above, I recommend that the authors use only two mineralogy, one with and one without garnet.

We have made amendments to Table 1 to improve clarity, including the addition of a colour scheme to highlight which mineral model is being used to calculate the different bulk D values. As explained above we wish to keep the full range of bulk D values calculated as this becomes important for later justification of the choice of partition coefficients.

Table 3 is also unclear: the favorite model might be the one shown in bold but this does not correspond to the text (EED007 instead of EED010); it is also unclear what explains the difference between consecutive lines (see lines 1 and 2, or lines 3 and 4, or lines 5 and 6). The D values differ but where do these D values come from and what does it imply? Please be clearer!

Firstly, the wrong line was inadvertently highlighted in table 3 – it should have been for the EED010 model. This has now been amended. We have also added a column to explain the key parameter change in each of the model runs and to link the lines in the table to the specific figures in the manuscript and supplement. We hope that this makes things clearer.

-paragraph starting with line 123. Why do you use the term harzburgite? From a petrology view point, this type of rock is "sterile". I think that you could simply use the term "peridotite".

This, somewhat unfortunate, terminology originates from this original modelling of this type by Christensen and Hoffman (1994). We have addressed this point significantly in response to the main points from Reviewer 1 and we have modified the main text and the supplementary information to clarify this.

Lines 139-141: please clarify! This has been reworded to – ‘To account for the above observations and following the method of Brandenburg et al. (2008) we model different eclogite excess densities (EED) ranging from 0% to 10% (i.e., EED=10% means that the eclogite tracers are 10% denser than the harzburgite tracers).’

-line 156-162: please provide a summary of the CC partition coefficients. The reader should not need to go and read carefully the Brandenburg et al. (2008) paper. Details of the CC partition coefficients – as stated in the manuscript they are simply set iteratively to produce the composition of the current continental crust. We added the following to improve clarification – ‘Full details of the values applied in different model cases are presented in Table S1. In general the retention coefficients for the parent species (Sm and Lu) are the higher than for the daughter species (Nd and Hf).’

-line 164: Th is not fluid-mobile!!!! The point that we are making here is that Brandenburg et al., (2008) considered Th to be fluid mobile in their modelling of continental crust formation. This is not something that we are implementing in the modelling conducted here. In addition, according to

Kessel et al., 2005 Th is fluid mobile under subduction zone temperature and pressure conditions. Therefore Th could be considered fluid mobile in relation to the formation of the continental crust.

-line 207-214: Where are the values in Table 3 or in Table 1? You mention values from Salters and Stracke for Lu and Hf but you do not specify if you selected the values calculated with residual garnet or the other set. This is the KEY for the final slope. The justification for the choice of parameters needs to be clearly expressed. We have specified the exact values in the text and have made Table 1 clearer.

-line 288-291: Here again give the KD values that you chose!! Completed.

-line 290-302: The argument about the calculated concentrations is a little weak. Values listed in Table 3 for the Nd and Hf upper mantle contents are very low (about ½ of primitive mantle) and the calculated concentrations for MORB are also very low (about 1/3 of the average MORB estimate). How do the authors explain the difference? Values that would be interesting to list in Table 3 are the concentrations of Sm and Lu but I doubt that the calculated Lu concentrations fit the MORB measured contents and the upper mantle estimates.

It appears that there was a problem with Table 3 – there was an error in the values displayed and the wrong values were underlined as being the closest to the concentrations of Hf and Nd in a MORB with 9 wt.% MgO (1.33 ppm Hf and 5.5 ppm Nd according to Jenner and O'Neill, 2012). We have reworked Table 3 and the correct values have now been used and highlighted.

The average concentration of the upper mantle (in our model considered to be at depths of between 100 km (i.e., below the melting zone) and 360 km) in our preferred model are 0.22 ppm for Hf and 0.88 ppm for Nd. Published concentrations for the primitive mantle are 0.227 ppm for Hf and 0.994 ppm for Nd (Lyubetskaya and Korenaga, 2007), and range up to higher values of 0.3 ppm for Hf and 1.327 ppm for Nd (Palme and O'Neill, 2003). Therefore we consider our model to provide a reasonable match to the concentrations that are expected for the upper mantle.

When calculating the MORB concentration we use the values of Jenner and O'Neill (2012) to obtain a concentration for a MORB with 9 wt.% MgO (so as to represent a primitive melt). This is indicated in the text and the calculation of the concentration for a 9 wt.% MgO melt is shown in supplementary Figure S4. This gives MORB concentrations (with 9 wt.% MgO) of 1.33 ppm for Hf and 5.5 ppm for Nd. For our preferred model a melt fraction of between 10 and 15% (implemented in batch melting equations) would give these concentrations, when using the upper mantle concentrations (explained above) and the implemented bulk D values (see Table 3). Higher concentrations (as observed with lower MgO wt.% - see Figure S4) would be produced by a lower melt fraction (see Table 3). We believe that this trace element information provides supporting information that the bulk D values we have chosen are not unreasonable.

The reason we only show the concentrations for Nd and Hf is that the elemental concentrations are calculated from the number of atoms of the isotope species. Therefore we need to have a good understanding as to the % of the element that is made up of a particular isotope. This value is most reliable for the stable isotope species (¹⁷⁷Hf and ¹⁴⁴Nd), therefore we have used these isotopes to calculate the elemental abundance for these trace elements.

-lines 303 down: in table 3, the highlighted line is EED007 and not EED010. Please check and clarify. The wrong line was indeed highlighted – this has now been amended.

Also strangely enough, the calculated field in figure 7a does not show the funnel shape due to continental crust recycling as demonstrated in figure 6. What is the explanation?

In figure 6 the bulk D values being used are still those from Workman and Hart (2005) for Sm and Nd, from Salters and Stracke (2004) for DMM at 2 GPa for Lu, and the adjusted value of 0.066 for Hf. In Figure 7 the bulk D values have been adjusted to generate more fractionation between the parent and the daughter isotope, this has had the effect of extending out the range of values so that the cone shape described is no longer observed. We have put 2 extra sentences in the manuscript to explain this (lines 323 - 326).

I would also recommend that the authors choose to plot the simulations as density plots (see plots in Chauvel et al. 2008). Such representation is much clearer in terms of representativity when producing magmas. Showing the age of the particle is very nice but this could be limited to the first figure showing how the simulations are done.

It is actually the depth of the tracer in the model that we are showing in plots such as Fig. 7a, not the age. We feel that this is the most important additional parameter to show as it shows what compositions are present in the upper mantle (i.e., to match the isotopic composition of the MORB source mantle) and what compositions are present in the lower mantle (i.e., to match the isotopic composition of the OIB source mantle). Whilst we agree that density plots can be a very useful way to show data, we don't believe it to be the most useful in this case where we are trying to compare the model results to the published geochemical dataset. Density plots of the geochemical data arrays will be strongly sample-biased to the places that have lots of measurements (like Hawaii, or some of the extreme mantle end-members). Also, the OIBs are not sampling the whole mantle, so it is unlikely that a PDF of the model output would match with a PDF plot of the geochemical data. Therefore, we believe that the way we are currently presenting the data – showing composition as a function of tracer depth is the most useful in identifying what compositions are in the MORB (i.e., upper mantle) and OIB (i.e., lower mantle) source and comparing them to the natural MORB-OIB dataset.

-lines 332 down: the arguments about the Archean mantle are very weak. Komatiites and basalts were formed then from a hot mantle and their HREE pattern are amazingly flat. Their Lu/Hf ratio is certainly not low

A recent paper by Gardener et al (2018) reported that the Archean felsic crust has lower Lu/Hf than that of the Proterozoic and Phanerozoic. We realise that we have caused some confusion here by not stating that this paper is referring to felsic crust, not Archean basalts. We have decided to remove this statement to avoid confusion and have emphasised the arguments outlined to the major comments above (e.g., see lines 337-355).

- lines 377-389: The model suggested here requires residual garnet when creating MORB, a suggestion that is not widely accepted in the community of geochemistry working with trace elements. This should be acknowledged and the trace element pattern of calculated MORB needs to be shown and compared to present day data. I encourage the authors to look at alternative models, in particular, models that would create the Lu/Hf fractionation during continental crust formation.

We accept that there is little evidence for a significant role for garnet in the MORB source region and that most melting occurs in the spinel field, particularly in the present day regime, although it may make up a small component as melting is established at a ridge (as supported by a comment made by Reviewer 1). And we are not suggesting that the MORB source (now or throughout Earth history) is dominated by a garnet bearing residuum, but the results of the modelling do suggest that we need a higher bulk D value for Lu to produce the epsilon Hf composition of the upper mantle. This implies that an increased role for at least a small amount of garnet in the melt source region in the early Earth compared to today. We have aimed to clarify this in the text (lines 337-355).

-lines 432 down: This part deserves a little more explanation. How much more recycling is needed to obtain average values similar to upper continental crust?

We have specified the exact values generated for the continental crust in the preferred model (Fig 7) (line 443). To match the average values for the upper continental crust ~200% of the present day continental crust has to be recycled into the mantle. This information has been added (lines 444-446).

-lines 461-465: This is your preferred interpretation but not necessarily reality. We agree – this is our preferred interpretation of the data. Hence we have reworded the sentence to – ‘In contrast, we interpret the results of the combined geodynamical-geochemical modelling presented here to suggest that the extraction, subduction (and/or delamination), and storage of oceanic crust in the lower mantle to be the key process driving the mantle-crust Lu-Hf and Sm-Nd systematics, with the formation and recycling of continental crust playing a lesser role.’

-figure 3: please label the various panels. Also provide explanation for what is plotted in panels e and f. Correspond to which line in Table 3? What is the residual mineralogy?

Additional information has been provided in the panels and in the Figure caption to give clarity on which residual mineralogies and bulk D values have been used. In addition, an extra column has been added to Table 1 to indicate, where possible, which figure 3 sub-figure corresponds with which bulk D values.

-figure 6 panels c and f: it would be nice to use a scale between 0 and 1 for the % of present-day crustal mass as done by Dhuime et al. among others

This is basically what is being shown in this figure, but we have used the overall mass of the continental crust as this fits better with information presented elsewhere in the paper (e.g., Table S1), instead of a scale between 0 and 1. To respond to this comment we have added a line on the graph to indicate the present day mass of the continental crust so that a % of the present day crustal mass at each time-step can be easily observed by the reader.

-- figure 7: why is there no spread at the unradiogenic end? In contradiction with figure 6. In response to an earlier comment this has now been explained in the text (lines 323 - 326). Please label panels b and c. We appreciate that labels are useful but it is difficult to include all the necessary text on the figure panel. We have provided a clear description in the figure caption.

-far too much supplementary material. Please make a selection. Readers will never look at them in detail. We feel that the supplementary information is important as it provides important details on the geodynamical and geochemical modelling. It essentially summarises the geodynamic model and provides clarifications on the geochemical model of Brandenburg et al (2008). Because our

modelling approaches are based on this former work, we do not feel it is appropriate to provide lengthy explanations in the main text; rather we provide summaries and references, with a lengthier explanation in the supplement for readers who are interested in the model details. We also provide the results of additional model runs for readers who want to check the sensitivity of the model to other parameters, which we are not able to discuss at length in the main manuscript.

-Table 1: see comments above. See responses to above comments – Table 1 has been amended and clarified.

-Table 3: this is where it appears that garnet must be residual. Lu has a much higher partition coefficient when garnet is residual than when it is not present. This is correct. We have modified Table 3 and inserted some additional lines of text to try to improve clarity (see also responses to earlier comments).

Highlights:

- Geodynamical model of mantle convection combined with TE and isotope geochemistry
- Model produces ϵ_{Hf} and ϵ_{Nd} values of the upper mantle and continental crust
- Enriched ocean island endmember compositions are also produced (e.g., EMI)
- First combined model to match both isotopic and trace element geochemistry
- Recycling and storage of oceanic crust in the deep mantle identified as key process

1 **Origins of the terrestrial Hf-Nd mantle array: evidence from a combined geodynamical-**
2 **geochemical approach**
3 Rosemary E. Jones^{1*}, Peter E. van Keken², Erik H. Hauri², Jonathan M. Tucker², Jeffrey Vervoort³, and
4 Chris J. Ballentine¹

5 ¹Department of Earth Sciences, University of Oxford, South Parks Road, Oxford, OX1 3AN, UK
6 ²Department of Terrestrial Magnetism, Carnegie Institution for Science, 5241 Broad Branch Road
7 NW, Washington DC 20015-1305, USA
8 ³School of the Environment, PO Box 642812, Washington State University, Pullman WA 99164-2812,
9 USA
10 *corresponding author. Email: Rosie.Jones@earth.ox.ac.uk Phone: +441865 272000

11
12 *Abstract*

13 The formation and segregation of oceanic and continental crust from the mantle, and its return to
14 the mantle via subduction and/or delamination, leads to the development of distinct geochemical
15 reservoirs in the terrestrial mantle. Fundamental questions remain regarding the location, nature,
16 and residence time of these reservoirs, as well as the respective roles of oceanic and continental
17 crust in the development of the mantle’s geochemical endmembers. The Lu-Hf and Sm-Nd isotope
18 systems behave similarly in magmatic systems and together form the terrestrial mantle Hf-Nd
19 isotopic array. Here we combine a geodynamic model of mantle convection with isotope and trace
20 element (TE) geochemistry to investigate the evolution of the Hf-Nd mantle array. This study
21 examines the sensitivity to: TE partition coefficients used in the formation of oceanic crust; density
22 contrasts between subducting oceanic crust and the mantle; and the formation and recycling of
23 continental crust. We show that that the fractionation between the parent (Lu and Sm) and
24 daughter (Hf and Nd) species needs to be higher than is indicated by partition coefficients
25 determined from the present-day melting environment. This is consistent with the suggestion of
26 deeper mantle melting earlier in Earth history and an increased role for residual garnet. [Subduction](#)
27 [and accumulation of](#) dense oceanic crust produces a large mass of incompatible TE enriched material
28 in the deep mantle. This deep mantle enrichment appears to play a more significant role than the

extraction and recycling of continental crust in developing the Hf and Nd isotope and TE compositions of the mid-ocean ridge mantle source. The corollary of this result is that the formation of the continental crust plays a secondary role, contrary to the currently accepted paradigm. Nevertheless, the inclusion of continental crust formation and recycling produces a broader model mantle array, which better reproduces the spread in the natural data set. This model also produces the Hf and Nd isotope and TE compositions of the upper mantle and continental crust, as well as deep mantle compositions similar to those of plume-fed ocean island basalts. Our model is consistent with continental growth models based on the Lu-Hf isotopic composition of zircon, which suggest that 50-70% of the present-day mass of the continental crust is produced prior to 3 Ga, and that the recycling of continental crust becomes more prevalent after this time.

1. Introduction

The chemical and isotopic evolution of the terrestrial mantle is largely influenced by the formation of oceanic crust (OC) at spreading ridges and continental crust (CC) through arc volcanism, and the subsequent recycling of this crust back into the mantle via subduction and/or delamination. These processes produce the geochemical heterogeneity observed in samples such as ocean island basalts (OIB) and mid-ocean ridge basalts (MORB) that are derived from different parts of the mantle. The coupled Lu-Hf and Sm-Nd isotope systems have provided key insights into the evolution of the mantle and crust over the course of Earth history (Salters and White, 1998; Vervoort and Blichert-Toft, 1999; Vervoort et al., 1999; Chauvel et al., 2008). The mineral-melt compatibility of the radioactive parent isotopes (^{176}Lu and ^{147}Sm) is greater than their daughter species (^{176}Hf and ^{143}Nd , respectively) resulting in the residual mantle becoming more radiogenic than the extracted crust over time. The relatively long half-lives of these systems (3.71×10^{10} yr for ^{176}Lu and 1.06×10^{11} yr for ^{147}Sm) compared to the age of the Earth, means that this isotopic divergence has been occurring over Earth history. Unlike U-Th-Pb, Lu-Hf and Sm-Nd are insensitive to redox conditions and relatively immobile in fluids, making these isotope systems ideal for investigating the dichotomy

between the formation and recycling of oceanic and continental crust in driving the geochemical evolution of the mantle. In addition, the high concentrations of Hf in the mineral zircon allows for the combined measurement of Hf isotopic compositions and U-Pb ages (e.g., Kinny and Maas, 2003; Fisher et al., 2014; Jones et al., 2015; Vervoort and Kemp, 2016). This makes the Lu-Hf isotope system key to the development of models of continental crustal growth, preservation, and recycling (e.g., Hawkesworth and Kemp, 2006; Belousova et al., 2010; Condie et al., 2011; Dhuime et al., 2012).

There is strong evidence that recycled crust is present in the deep mantle and influences the source of plume-fed ocean islands (White, 2015 and references therein). OIBs have a wide range of isotopic compositions, which have been grouped into different categories (e.g., EMI, EMII, and HIMU White, 1985; Zindler and Hart, 1986; Stracke et al., 2005). ‘Enriched’ mantle (EM) endmember compositions are enriched in incompatible trace elements relative to MORB and are divided into two groups. EMI compositions have primarily been linked with the recycling of sediments (e.g., Weaver, 1991; Eisele et al., 2002), lower continental crust (Willbold and Stracke, 2006, 2010), or metasomatised subcontinental lithosphere (e.g., Zindler and Hart, 1986; Tatsumoto et al., 1992). EMII compositions have been attributed to the presence of small quantities of recycled terrigenous sediment (e.g., Zindler and Hart, 1986; Chauvel et al., 1992). HIMU OIBs are related to recycled oceanic crust, that has either had Pb preferentially removed by seafloor alteration and/or slab dehydration during subduction (e.g., Weaver, 1991; Chauvel et al., 1992; Peucker-Ehrenbrink et al., 1994; Kogiso et al., 1997) or has been enriched in U due to interaction with U-rich continental sediments after ~2 Ga (Elliott et al., 1999; Hanyu et al., 2014). The source of mid-ocean ridge basalts (MORB) is referred to as the depleted MORB mantle (DMM) reflecting its chemical depletion in incompatible TE as a result of upper mantle melting and crust formation.

Mass balance modelling is a useful way to investigate the geochemical evolution of the Earth. The resulting ‘box models’ provide some constraints on the relative interactions between reservoirs and

the role of crust formation and recycling (e.g., Jacobsen and Wasserburg, 1979; Allègre and Lewin, 1995; Albarède, 1998; Coltice and Ricard, 1999; Kumari et al., 2016). Such studies can be further enhanced by full geodynamical modelling that can incorporate more realistic estimates on the rate of oceanic crust formation (which depends on plate velocities) and the subsequent remixing upon recycling (which depends on convective vigour), in turn controlled by the viscosity structure of the Earth's mantle. Christensen and Hofmann (1994) were the first to combine geodynamical modelling with geochemistry. They used a 2D Cartesian convection model to investigate the terrestrial U-Pb and Sm-Nd systems and found that extraction, recycling, and storage of oceanic crust in the deep mantle produced MORB-HIMU trends over 3.6 Byr. These early geophysical-geochemical model studies (see also Davies, 2002) imposed plate motions, and the recycling and remixing of oceanic crust were strongly influenced by these kinematic boundary conditions. Full dynamical models (e.g., Xie and Tackley, 2004; Brandenburg and van Keken, 2007) avoid the strong influence of external forcing through the boundary conditions and are more appropriate tools to study convective mixing in the Earth's mantle.

The combined geodynamical-geochemical model used in this study is based on an updated version of the model by Brandenburg et al. (2008). This mantle convection model uses a 2D cylindrical geometry with a reduced core radius to better match the heat flow characteristics of the spherical Earth (van Keken, 2001). It incorporates plate tectonics through a force-balanced plate method, which causes plate movement in an energy-conservative manner. It reproduces some key physical features of plate tectonics and mantle convection including: a match to the present day heat flow and plate velocities (Brandenburg et al., 2008); sinking slab geometries that show similarities to mantle tomography (Van der Hilst et al., 1997; Ritsema et al., 2011; see van Keken, 2013 for a direct comparison); and accumulation of oceanic crust near the core-mantle boundary (CMB) (e.g., Spasojevic et al., 2010). The resulting models also satisfy key geochemical constraints with a more heterogeneous lower mantle preserved below a [well-stirred](#) upper mantle (Hofmann, 1997) and reproduce the observed geochemical distribution in multiple isotope systems (U-Th-Pb, Rb-Sr, Sm-

Nd, and Re-Os) that define the DMM, HIMU, and EMI mantle endmembers (Brandenburg et al., 2008).

In this study, we extend this model to include the Lu-Hf isotope system and focus in particular on its co-evolution with Sm-Nd. During mantle melting, Hf and Nd are more incompatible than Lu and Sm and hence a greater proportion of these elements are partitioned into the melt and, therefore, to the newly generated crust. The Hf and Nd isotopic compositions are often expressed as epsilon (ϵ) values, where ϵ represents the deviation of the Hf and Nd isotope compositions ($^{176}\text{Hf}/^{177}\text{Hf}$ and $^{143}\text{Nd}/^{144}\text{Nd}$) of the material of interest relative to that of the chondritic reservoir (CHUR), measured in parts per ten thousand. The ϵ_{Hf} and ϵ_{Nd} compositions of OIB and MORB display a linear relationship, known as the mantle array (e.g., Vervoort et al., 1999) (Fig. 1). In this array the DMM shows positive ϵ_{Hf} and ϵ_{Nd} values and enriched mantle compositions (EMI, EMII) extend to negative ϵ_{Hf} and ϵ_{Nd} compositions. Average continental crust compositions are even more negative (upper CC: $\epsilon_{\text{Hf}} = -13.2 \pm 2.0$, and $\epsilon_{\text{Nd}} = -10.3 \pm 1.2$; Chauvel et al., 2014) and HIMU compositions lie slightly below the array with more negative ϵ_{Hf} relative to ϵ_{Nd} values (Fig. 1).

2. Geodynamical-geochemical model methods

Our models closely follow the modelling presented in Brandenburg et al. (2008). We use the same geodynamical models produced from finite element modelling. The geochemical modelling, which is performed as a post-processing step, is extended to investigate the Lu-Hf and Sm-Nd systems. We provide a brief description of our methods below and a more complete description in the Supplementary Information. A schematic representation is presented in Figure 2.

We mimic the physical process of mid-oceanic ridge melting by batch melting of a small volume of mantle in the regions where plates diverge. In the geodynamical models we use this melting to separate a basaltic crust and harzburgitic residue from peridotite. In the geochemical modelling we incorporate the effects of redistribution of isotope species during batch melting. In both cases we

use the formulation of Christensen and Hofmann (1994) with an initial mantle composition of undepleted peridotite (bulk silicate earth (BSE) (McDonough and Sun, 1995)). We represent the peridotite lithology with two components that we call (following Christensen and Hofmann, 1994) 'eclogite' and 'harzburgite'. While recognizing that the terms 'eclogite' and 'harzburgite' are mineralogical terms that are valid only in the upper mantle, we note that we do not model any phase changes in the mineral assemblages. As a consequence, we will, with apologies to the reader, refer to any tracer that melts to form OC as 'eclogite' and any tracer that is part of the residue during melting as 'harzburgite' irrespective of their position in the model. Upon melting the active eclogite tracers are physically repositioned at the surface to form new OC (Fig. 2). This approach allows us to dynamically investigate the role of OC recycling on the dynamics of the mantle and its geochemical evolution. At depth, the OC is denser than the surrounding mantle by 3 – 7 % in the upper mantle (Irifune, 1987; Ringwood, 1990; Aoki and Takahashi, 2004) and 0.5 – 5 % in the lower mantle (Kesson et al., 1994; Hirose et al., 2005; Ono et al., 2005; Ricolleau et al., 2010). We use the geodynamical models of Brandenburg et al. (2008), which use a range of 0% to 10% of eclogite excess densities (EED), where an EED of 10% means that the eclogite tracers are 10% denser than the harzburgite tracers.

In the geochemical model, melting events are accumulated in 5 Myr intervals such that we have a sufficiently large number of tracers available for the batch melting calculations. We compute the total number of atoms of each isotope of interest by summing the atoms present in the melt zone. We define a melt fraction (f) based on the relative volume of the combined eclogite tracers to total volume. This is a simple first-order parameterization of melting at a mid-oceanic ridge where we will assume the melt fraction on average is 12.5 % (e.g., McKenzie and Bickle, 1988). The eclogite tracers on average represent 12.5 % of the mantle. During the model evolution the melt fraction varies around this fraction due to stochastic changes in the relative number of eclogite and harzburgite tracers for the EED=0% case. For the cases with higher EED, an increasing number of eclogite tracers tend to remain in the deep lower mantle, and this reduces f by a few % over the course of the model

run. We employ batch melting equations using the computed f and selected partition coefficients to find the composition of the melt and residue. We then distribute the number of atoms in the melt equally between the eclogite tracers (thereby enriching them in incompatible elements) and distribute the atoms in the residue equally over the harzburgite tracers in the melt zone. We implement a number of published bulk D values in the model (Kelemen et al., 2003; Salters and Stracke, 2004; Workman and Hart, 2005), which are primarily derived from natural samples and selected in order to reflect large-scale global processes. Salters and Stracke (2004) present different K_d and mineral abundances for different pressures (2 and 3 GPa; representing depths of melting), resulting in large variations in the bulk D values produced for each element (Table 1).

In models where we simulate the formation of continental crust (CC), we further extract atoms from the recently melted eclogite tracers and store these in an extant CC reservoir. For this we use a separate set of partition coefficients. In Brandenburg et al. (2008) these were termed ‘extraction coefficients’ but, in an unfortunate error, the paper listed values for these coefficients that were actually the relative amount of atoms retained in the eclogite tracers, not that extracted to the CC. To be able to compare these coefficients with the previous paper we will list the relative amount retained as ‘retention’ coefficients. Newton iteration is used to determine the retention coefficients required to produce the present-day composition (Rudnick and Gao, 2014) and mass of the CC (2.4×10^{25} g) (CC_{pd}).

In the preferred geochemical models of Brandenburg et al. (2008), two sets of retention coefficients were applied to fluid-mobile elements (Pb, Th, Rb), before and after a somewhat arbitrary age of 2.25 Ga. This follows guidance from earlier box modelling (Rudge et al., 2005; Kellogg et al., 2007; and later by Kumari et al., 2016) and is required to provide a better fit between models and observations, in particular to Pb isotope data. As the trace elements considered here (Lu, Hf, Sm, Nd) are relatively immobile in fluids (Kessel et al., 2005), only one set of retention coefficients is applied. CC production starts at 4.0 Ga based on the age of the oldest continental crust (e.g., Bowring and

Williams, 1999). The CC composition changes due to continued addition by CC extraction from the eclogite tracers and radiogenic ingrowth. We allow for the optional recycling of this evolving CC back into the mantle, potentially reflecting subduction erosion, delamination of the CC and/or the subduction of continentally derived sediments. When this functionality is applied, a fraction of the number of atoms of each isotope species (e.g., ^{176}Lu , ^{176}Hf , ^{177}Hf , ^{147}Sm , ^{143}Nd , ^{144}Nd), contained in the CC at a particular time interval, is removed and distributed to each eclogite tracer that has just participated in a melting event (i.e., newly formed OC).

3. Modelling approach and results

3.1 Approach

A step-wise approach was implemented to test the sensitivities of the Lu-Hf and Sm-Nd isotope systems to different variables and starting conditions, with increased complexity gradually built into the model. The aim of the modelling was to produce the composition of the present-day upper mantle (UM) ($\epsilon_{\text{Hf}} = \sim 14\text{-}18$ and $\epsilon_{\text{Nd}} = \sim 9\text{-}10$; White and Hofmann, 1982; Vervoort and Blichert-Toft, 1999; Chauvel and Blichert-Toft, 2001; Salters and Stracke, 2004; Workman and Hart, 2005), OIB endmembers, and CC (upper CC: $\epsilon_{\text{Hf}} = -13.2 \pm 2.0$, and $\epsilon_{\text{Nd}} = -10.3 \pm 1.2$; Chauvel et al., 2014), as well as the slope of the Hf-Nd mantle array (Fig. 1). The geochemical model parameters that remained constant are presented in Table 2.

3.2 Sensitivity to prescribed partition coefficients

We first tested the model sensitivity to different choices of partition coefficients (Fig. 3). The bulk D values of Workman and Hart (2005) produce a range of ϵ_{Hf} values that far exceed the range in the global dataset (+53 to -24 for EED=10%, Fig. 3a). The bulk D values calculated using the mineral/melt partition coefficients (K_d) of Kelemen et al. (2003) and Salters and Stracke (2004) (for DMM at 2 GPa; Table 1) produce a much better fit to the global ϵ_{Hf} dataset (Fig. 3b and c). However, the opposite is the case for ϵ_{Nd} , and in this case the bulk D values of Workman and Hart (2005) result in a better

match (values ranging between +15 and -6, Fig. 3a), particularly in comparison to Salters and Stracke (2004) values for 2 GPa (Fig. 3c).

Kd values from Salters and Stracke (2004) for melting at 3 GPa produce a range of ϵ_{Hf} values that extend to much wider values than the global dataset (+59 to -47) and also result in the slope of the generated $\epsilon_{\text{Hf}}-\epsilon_{\text{Nd}}$ array being far too steep (Fig. 3d). This is related to Lu being highly compatible in garnet (Table 1), which is present during mantle melting at higher pressures, resulting in a greater fractionation between Lu and Hf (i.e., $D_{\text{Lu}}/D_{\text{Hf}}$, Table 1), with less Lu being partitioned into the melt.

The published partition coefficients that best match the spread and slope of the Hf-Nd mantle array are those of Workman and Hart (2005) for Sm (0.045) and Nd (0.031) combined with those for DMM at 2 GPa (i.e., without garnet) from Salters and Stracke (2004) for Lu (0.137) and Hf (0.061) (Table 1, Fig. 3). A slight improvement on the fit can be achieved by adjusting the bulk D value for Hf to 0.066 (Fig. 3f). Bulk D values vary as a function of pressure and mineral abundance. As melting in the model extends to depths of 100 km, and as the mineral abundances in the mantle are likely to have changed over time, we consider adjusting the bulk D values within the range of those published (Table 1) to be realistic for the purposes of this large temporal and spatial scale modelling.

3.3 The effect of excess eclogite (EED) density

In the second stage of modelling we investigated the effect of changing EED on the geochemical evolution using the preferred bulk D values detailed above (Figs 4, 5, and S1). In the neutral buoyancy case, the spread in Hf and Nd isotope compositions is more restricted than the global data array (Fig. 4a). There is also little variability in composition with depth and time (Fig. 4d) and the model is far from reproducing the ϵ_{Hf} and ϵ_{Nd} compositions of the UM, with average values of 1.0 and 0.7. As the EED increases the spread in the ϵ_{Hf} and ϵ_{Nd} values produced by the model also increases and more variability is observed with depth and time (Fig. 4). A notable feature is the development of increasingly unradiogenic Hf and Nd isotope compositions in the deep mantle. This

reflects the accumulation of subducted eclogite at the CMB. The preferential partitioning of the daughter species (Hf and Nd) into eclogite results in the deeply stored OC developing less radiogenic compositions over time. With higher EED, more OC is stored at the CMB and more extreme negative ϵ_{Hf} and ϵ_{Nd} compositions develop (Figs. 4 and 5). The average ϵ_{Hf} and ϵ_{Nd} values in the deepest mantle in the EED=10% model are -13.6 and -4.4. Conversely, the harzburgite tracers are relatively enriched in the parent isotopes (^{176}Lu and ^{147}Sm) and develop radiogenic Hf and Nd compositions over time. Areas of the mantle that contain a higher proportion of harzburgite compared to eclogite have positive ϵ_{Hf} and ϵ_{Nd} , as is reflected in the composition of the UM (Figs. 4 and 5). The accumulation of eclogite tracers in the deep mantle is also demonstrated by the higher concentrations of incompatible TE near the CMB, which becomes more prevalent in the higher EED models (Figs. 5d-f).

Although the simple production, recycling, and storing of OC in the model produces a good fit between the model data and the global data array (e.g., Fig. 4b), it fails to reproduce the Hf and Nd isotope compositions of the UM. Even the most extreme EED model (EED=10%) has average UM ϵ_{Hf} and ϵ_{Nd} compositions of only +6.3 and +3.0 respectively (Fig. 4c and f).

3.4 The production and recycling of continental crust

In the third stage of modelling we tested the effects of producing and recycling of continental crust (CC). The retention coefficients implemented change depending on the EED, partition coefficients, and whether CC is recycled (Table S1). Here, we focus on the 10% EED model (Fig. 6), as it produces UM compositions that are closest to the observed values (Section 3.3). The results from the production and recycling of CC in the EED=0% and EED=7% models are shown in Supplementary Figures S2 and S3.

The generation of CC in the model ($1 \times \text{CC}_{\text{pd}}$ extracted) produces a slightly more restricted and positive data array with a broader spread in Hf isotope compositions (Fig. 6a compared to 4c). The

composition of the lower mantle does not evolve to such unradiogenic Hf isotope compositions, with a maximum final ϵ_{Hf} of -10.2 compared to -13.6 without CC extraction (Fig. 6b compared to 4f). This is due to the preferential extraction of incompatible TE into the CC, forming a competing, unradiogenic and negative ϵ_{Hf} and ϵ_{Nd} reservoir over time. As a result of this depletion, the rest of the mantle becomes more radiogenic in its Hf and Nd isotope composition (above 2500 km in Fig. 6b).

Dhuime et al. (2012) suggested that 100% of the present volume of the CC has been destroyed and recycled back into the mantle since 3 Ga. We simulated this by producing, over time, twice the present-day mass of the CC and recycling one mass back into the mantle from 4.05 Ga ($2 \times \text{CC}_{\text{pd}}$ extracted, $1 \times \text{CC}_{\text{pd}}$ recycled). This generates more unradiogenic Hf and Nd isotope compositions in the lower mantle (below 660 km) and a Hf-Nd isotope array with a wider spread (Figs. 6d and e). As recycled CC is carried by the eclogite tracers, it follows their movement in the geodynamical model and is potentially stored in the deep mantle, producing greater compositional heterogeneity (Fig. 6d). Although recycling CC generates more heterogeneity, the average Hf and Nd isotope compositions of the UM and at the CMB are similar to those produced without CC recycling (Figs. 6b and e). The recycling of CC produces more realistic Hf and Nd isotope compositions for the CC itself (ϵ_{Hf} and ϵ_{Nd} of -24 and -17, respectively) compared to the case without CC recycling (-33 and -22) (Figs. 6b and e). Since we keep the [proportion of the CC recycled](#) constant over model time, the CC extracted early in the model run that evolves to highly unradiogenic compositions is redistributed into the mantle via the eclogite tracers. This results in a CC that evolves to less extremely negative ϵ_{Hf} and ϵ_{Nd} compositions. Additionally, the growth of the CC without CC recycling is nearly linear (Fig. 6c). In contrast, when CC is recycled, the continental growth curve is initially steep and then shallows implying that recycling becomes a more prevalent process over time (Fig. 6f). The latter qualitatively matches some of the proposed models for the growth of the CC primarily based on Hf isotopic compositions of zircons (e.g., Belousova et al., 2010; Dhuime et al., 2012).

The extraction and recycling of CC does generate more positive ϵ_{Hf} and ϵ_{Nd} compositions (+6 and +3) in the UM, compared to models without CC formation, but these still differ from the observed values. This suggests that the UM is not being sufficiently depleted in the daughter isotope relative to the parent isotope (i.e., $D_{\text{Sm}}/D_{\text{Nd}}$ and $D_{\text{Lu}}/D_{\text{Hf}}$ are too low) to develop more radiogenic Hf and Nd isotope compositions.

3.5 Re-assessing the prescribed partition coefficients

The models presented thus far fail to produce the observed radiogenic Hf and Nd isotope composition of the UM. In order to generate a complementary unradiogenic reservoir, the fractionation between the parent and daughter species could be changed to retain more Lu and Sm relative to Hf and Nd in the melting residue (harzburgite tracers). This would lead to more radiogenic Hf and Nd isotope compositions in the harzburgite and less radiogenic compositions in the eclogite. The spread and slope of the Hf-Nd isotope array is governed by $(D_{\text{Lu}}/D_{\text{Hf}})/(D_{\text{Sm}}/D_{\text{Nd}})$. The only satisfactory way we found to produce the Hf and Nd isotope compositions of the UM, and the slope of the Hf-Nd mantle array, was to adjust the bulk D values to increase the fractionation between the parent and daughter species. In the preferred model, the bulk D values used are $\text{Sm}=0.067$, $\text{Nd}=0.015$, $\text{Lu}=0.464$ and $\text{Hf}=0.048$ (Table 3), all of which are still within the range of the published values (Table 1). However, we recognize there is an immediate influence of the way we compute the melt fraction in the model, and therefore, our resulting preferred bulk D values are not necessarily representative of 'true' bulk D values.

To further ensure that the assigned bulk D values are not unrealistic, we applied batch melting to the average composition of the UM just below the depth of the melting zone (100-360 km) to check that the melt generated has a TE composition similar to MORB (Jenner and O'Neill, 2012, Supplementary Figure S4). A good match is seen between the TE composition of batch melts produced from the average UM in the model with a melt fraction of between 10 and 15% and MORB composition with 9 wt.% MgO (Table 3). Increasing the EED depletes the UM in TE more strongly, due to increased

storage of eclogite at the CMB. We also tested the sensitivity of the model to different BSE compositions. For example, the BSE concentrations of Palme and O'Neill (2003) are higher for Lu, Hf, Sm and Nd compared to McDonough and Sun (1995). When these concentrations are utilised this also results in a more TE-enriched UM and, in this case, the composition of a MORB with 9 wt.% MgO is matched with a higher melt fraction (Table 3).

The results of our preferred model are presented in Figure 7. To reproduce the Hf and Nd isotope compositions of the UM (Figs. 7b and c) the range of values throughout the mantle exceeds those exhibited in the Hf-Nd mantle array (Fig. 7a). Specifically, the values observed in the lower mantle spread to compositions not measured in OIB samples that are thought to be sourced from the lower mantle. The model lower mantle at the CMB has an average ϵ_{Hf} composition of -38 and ϵ_{Nd} of -14. The mantle above 2500 km depth has average compositions more radiogenic than CHUR (Bouvier et al., 2008), with the depleted UM showing the most positive ϵ_{Hf} and ϵ_{Nd} compositions of 12–18 and 7–10 respectively (Fig. 7). Without the production and recycling of CC (Fig. S5) the lower mantle evolves to similarly negative ϵ_{Hf} and ϵ_{Nd} values (-37 and -15), but the mantle above 2500 km depth evolves to less radiogenic compositions with the UM falling short of the DMM composition ($\epsilon_{\text{Hf}} = 12$, $\epsilon_{\text{Nd}} = 6$) (Table 3).

We note that the shape of the Hf and Nd isotope array produced by the preferred model is more curved than the measured array, but that the center of the model array overlaps the mantle array and the model produces compositions that match the DMM, FOZO, and EM mantle endmembers (Fig. 7). The increased curvature is primarily caused by the trajectory in the model array that has higher ϵ_{Nd} than ϵ_{Hf} values. These compositions reflect the presence of ultra-depleted harzburgitic tracers, which have participated in more than one mantle melting event. In addition, as a result of the adjustment of the partition coefficients, the Hf-Nd array loses the 'cone-like' shape shown in Figure 6d. This is due to the adjusted partition coefficients extending the values in the array to more extreme values, which reduces the apparent effect of CC recycling.

4. Discussion

4.1 Sensitivity to partition coefficients

The results of the geodynamical-geochemical model are highly sensitive to the prescribed bulk D values (much more so than to melt fraction, shown in Table 3 and Figure S9). Parent and daughter species have different compatibilities in different mantle minerals, and therefore the Lu/Hf and Sm/Nd of the melt is controlled by the minerals present in the source. Lu has a much higher compatibility in garnet (and somewhat higher in clinopyroxene) than Hf (Table 1), meaning the presence of even a small amount of garnet (typically stable at $P > 1$ GPa) in the melt source region would result in a lower amount of Lu, relative to Hf being partitioned into the OC. Similarly, Sm has a higher compatibility in garnet and clinopyroxene compared to Nd.

Present day MORBs are thought to be primarily produced from melting in the spinel stability field (<60 km depth) and there is likely to be little garnet present. However, the abundance of certain mineral phases in the melt source region, and which stability field (garnet versus spinel and plagioclase) melting occurred in, has likely changed over the course of Earth history. The Archean mantle is widely considered to be hotter than the modern mantle (e.g., Herzberg et al., 2010 and references therein), which would have resulted in a higher degree of partial melting and the production of a thicker, warmer, and more buoyant OC (e.g., Sleep and Windley, 1982; Bickle, 1986). In our preferred model the partition coefficients were adjusted to increase the fractionation between the parent (Lu and Sm) and daughter (Hf and Nd) species. This could be accounted for by the presence of residual garnet in the melt source region in the early Earth when melting may have occurred at deeper levels, due to the thickness of the overlying crust. Salters and Hart (1989) also suggested that the Lu–Hf and Sm–Nd systematics of MORBs requires garnet to be a residual phase in melt genesis, and proposed a model in which melting starts in the garnet stability field and then continues at shallower levels. Hirschmann and Stolper (1996), alternatively, propose that the combination of spinel peridotite with 3–6% pyroxenite, with $\geq 20\%$ modal garnet, could also account

for the Lu–Hf and Sm–Nd compositions of most MORB. Our model supports an increased role for garnet and, overall, suggests that elemental partition coefficients, combined with present-day MORB source mineral abundances and melt fractions, may not be appropriate for the entirety of Earth evolution.

The adjusted partition coefficients in the preferred model produce a range of Hf and Nd isotope compositions not observed in the MORB-OIB mantle array (Fig. 7a). However, extremely high ϵ_{Hf} and ϵ_{Nd} values (60 and 21 respectively) have been reported for abyssal peridotites that represent residual mantle (Stracke et al., 2011). These compositions have been attributed to ancient mantle depletion, with the comparatively unradiogenic Nd isotope compositions reflecting higher susceptibility to resetting by melt-rock interaction of Sm–Nd compared to Lu–Hf. A number of studies have also suggested that the mantle is more heterogeneous in composition and contains more extreme isotopic compositions than have been measured in MORB and OIB to date (e.g., Bizimis et al., 2007; Liu et al., 2008; Stracke et al., 2011). This is consistent with the model results presented here. The extreme isotopic compositions contained in portions of the residual mantle are unlikely to be reflected in MORB and OIB compositions, as these domains are refractory and thus contribute little to the genesis of magmas, and their compositions are easily overprinted by melting of more TE enriched, fertile portions of the mantle.

A recent study has reported chondritic Hf isotopic compositions of Eoarchean zircons and interpreted this as evidence that there was no early, planet-scale depletion of the mantle in the Hf isotope record prior to 3.8 Ga (Fisher and Vervoort, 2018). We tested this scenario of late stage mantle depletion and found negligible impact on the geochemical evolution (Table 3, Fig. S8). The ϵ_{Hf} and ϵ_{Nd} compositions obtained for the upper mantle were slightly lower than observed, but a match could be made by further adjustment of the model partition coefficients.

4.2 Variations with depth and the development of OIB endmember compositions

The least radiogenic Hf and Nd isotope compositions in all results are found in eclogite that experienced melting early and was subducted and stored in the deep mantle (Figs. 3 - 7). Increasing EED results in increasingly unradiogenic Hf and Nd isotope compositions (Fig. 4), as more eclogite is retained near the CMB. The negative ϵ_{Hf} and ϵ_{Nd} region of the mantle array is occupied by the enriched mantle compositions such as those obtained for EMI and EMII OIBs. These EM compositions have been linked with the recycling of sediments, delaminated lower CC, or metasomatised subcontinental lithosphere (e.g., Zindler and Hart, 1986; Weaver, 1991; Chauvel et al., 1992; Tatsumoto et al., 1992; Eisele et al., 2002; Willbold and Stracke, 2006, 2010). The results presented here suggest that the incorporation of OC recycled into the source of OIBs could partly account for the EM compositions.

The results also support, in part, the conclusions of earlier combined geodynamical-geochemical models (e.g., Christensen and Hofmann, 1994; Davies, 2002; Xie and Tackley, 2004; Brandenburg et al., 2008), which suggested that the pooling of dense OC at the CMB plays a fundamental role in developing MORB and OIB compositions. These previous studies, however, tended to focus on the U-Th-Pb isotope systems and the development of HIMU mantle compositions. In this study we do not produce HIMU and extreme EMII Hf and Nd isotope compositions, suggesting that a geochemical component, such as recycled oceanic sediments, is missing. Chauvel et al. (2008) suggested that the Hf-Nd mantle array cannot be produced from the recycling of basaltic OC alone and invoked the need for recycling of both OC and sediments (over 3 Byr) into the source of OIBs to produce MORB-OIB compositions. *In contrast, our model results show that a large proportion of the Hf-Nd mantle array can be produced by the recycling of OC alone (Fig. S5). Producing and recycling CC produces a wider spread in the Hf-Nd isotope array (Fig. 7), but recycling oceanic sediments into the mantle, which have a shallower Hf-Nd isotope array (Chauvel et al., 2008) (not modelled here), may be required to generate the full array (i.e., HIMU and extreme EMII compositions).*

The extreme unradiogenic Hf and Nd isotope compositions produced in the lower mantle of the preferred model (Fig. 7a) are not observed in natural samples (Fig. 1). However, the isotopic compositions of the plumes rising in the model show a mixture of material being entrained into them with a range of compositions. Therefore, the less extreme compositions observed in OIB might reflect the mixing of recycled OC with more residual portions of the mantle, or mantle which has not undergone melting (e.g., Li et al., 2014), both of which would have more radiogenic Hf and Nd isotope compositions.

4.3 The growth of the continental crust

The formation of the CC in the model is rather simplistic and involves the extraction of incompatible TE from the eclogite tracers based on iteratively set retention coefficients. In the Earth this might reflect the formation of early CC from basaltic crust and subduction zone processes involving the dehydration and melting of down-going OC (e.g., Zegers and van Keken, 2001; Johnson et al., 2017; Gardiner et al., 2018). Although we set the retention coefficients arbitrarily, the values used in the preferred model (Table S1) generally mirror melt/mineral and fluid/mineral (Kessel et al., 2005) partitioning behaviour, with preferentially higher extraction of Hf and Nd into the CC compared to Lu and Sm.

Early geochemical models suggested that the formation of the CC is critical in developing the composition of the depleted mantle (e.g., Jacobsen and Wasserburg, 1979; Hofmann, 1988; McCulloch and Bennett, 1994; Workman and Hart, 2005). In our preferred model the production and recycling of the CC has a limited effect in terms of matching the composition of the present-day UM, OIB endmembers, and the slope of the Hf-Nd mantle array (Figure S5 shows the result without CC extraction and recycling). Instead, the formation, recycling, and critically the storage of OC near the CMB is found to be the more important process in determining the mantle and crustal Lu-Hf and Sm-Nd compositions. The mass of the OC produced in the model (2.83×10^{26} g, assuming a constant rate of production for 4.55 Byr) is considerably greater than the mass of CC produced in the model

(2.40×10^{25} g, or 4.8×10^{25} g if one mass of the CC is recycled). Despite the higher enrichment of the CC in incompatible TE compared to the OC, the large mass of recycled OC stored in the deep mantle (with increased EED), which is also a longer-lived reservoir than the CC, provides a more effective mechanism of sequestering incompatible TE from the convecting mantle. This is supported by the TE composition of the UM produced in the model with and without the formation of CC. When CC is formed in the model, the UM is only marginally more depleted, and subsequently produces the composition of MORB (9 wt.% MgO) with a slightly lower melt fraction (Table 3).

The Hf and Nd isotope composition of the CC generated in the model more closely matches the average composition of the upper CC (Chauvel et al., 2014) when continental crust is recycled in the model (Fig. 6e). Without CC recycling the models develop average compositions that are too extreme due to the long residence time of the earliest formed CC (4.05 Ga) (Fig. 6b). Recycling continental crust into the mantle, which could occur through subduction of continental sediments, subduction erosion of continental crust, or delamination of thick continental crust, reduces the average Hf and Nd isotope compositions developed in the model CC. Thus our model lends support to the hypothesis that a volume of CC, equal to the present day volume of the continents, may have been recycled into the mantle over geological time (e.g., Dhuime et al., 2012). The final Hf and Nd isotope compositions obtained for the CC, even when continental recycling is implemented in the model, are still less radiogenic ($\epsilon_{\text{Hf}} = -19.5$ and $\epsilon_{\text{Nd}} = -14.2$) than the values proposed for the average upper CC ($\epsilon_{\text{Hf}} = -13.2 \pm 2.0$, and $\epsilon_{\text{Nd}} = -10.3 \pm 1.2$ (Chauvel et al., 2014)). In order to generate the composition of the average upper continental crust, 200% of the present day mass of the CC would have to be recycled into the mantle. However, as no average ϵ_{Hf} and ϵ_{Nd} values have been proposed for the mid to lower CC, which may include a significant mass of older crust with lower ϵ_{Hf} and ϵ_{Nd} , we consider the more negative ϵ_{Hf} and ϵ_{Nd} values obtained for the CC in our preferred model (Fig. 7b and c) to be suitably realistic.

Different workers have suggested different models for the growth of the continental crust, including early formation (Armstrong, 1981), episodic growth (e.g., Condie and Aster, 2010) and relatively late stage formation (after 2.5 Ga) (e.g., Allègre and Rousseau, 1984; for a review see Hawkesworth et al., 2019). Our results with CC recycling lead to a CC growth curve similar to those suggested by Belousova et al. (2010) and Dhuime et al. (2012), based on Hf isotopic compositions of zircons combined with U-Pb ages (Fig. 6f). These growth curves suggest that a mass equivalent to 50-70% of the current CC mass was accumulated prior to 3 Ga. These studies go on to suggest that crustal recycling and reworking dominated over juvenile additions to the continental crust since at least the end of the Archean (2.5 Ga), possibly related to the onset of subduction-driven plate tectonics (Dhuime et al., 2012).

5. Conclusions

Our preferred model (based on excess eclogite density of 10%, with production and recycling of continental crust (CC), and adjusted bulk D values suggesting an increased role for residual garnet during mantle melting) reproduces the Hf and Nd isotope compositions of the upper mantle and continental crust. Negative ϵ_{Hf} and ϵ_{Nd} are consistently observed in the lower mantle in all model results and are caused by subducted and deeply accumulated oceanic crust. These compositions are similar to OIB enriched mantle endmembers (EMI and EMII), suggesting they are derived from the deep mantle. To generate the trace element depleted and radiogenic Hf and Nd isotope compositions of the upper mantle, the Earth must have a mechanism of generating and preserving a trace element (TE) enriched and unradiogenic Hf and Nd isotope reservoir somewhere in the mantle or crust. Previous geochemical studies have suggested the extraction of the continental crust is a critical process in generating the TE and isotopic composition of the upper mantle (e.g., Hofmann, 1988; McCulloch and Bennett, 1994; Workman and Hart, 2005). In contrast, we interpret the results of the combined geodynamical-geochemical modelling presented here to suggest that the extraction, subduction (and/or delamination), and critically the storage of oceanic crust in the lower

mantle to be the key process driving the mantle-crust Lu-Hf and Sm-Nd systematics, with the formation and recycling of continental crust playing a lesser role. [We suggest that the accumulation of recycled oceanic crust in the deep mantle provides a more effective mechanism of sequestering incompatible TE from the convecting mantle than the continental crust.](#) This conclusion is reached based on the model reproducing both TE abundances and isotopic compositions of the upper mantle (DMM). The match to upper mantle compositions and the Hf-Nd mantle array is improved with CC production and recycling. The growth of the CC in the model is consistent with the continental growth curves based on Hf isotopic signatures obtained from zircon (Belousova et al., 2010; Dhuime et al., 2012), suggesting the growth of the continental crust is not a linear process through a simple steady-state extraction from the mantle. Including the recycling of oceanic sediments, which produce a shallower Hf and Nd isotope array (Chauvel et al., 2008), could extend the spread of the data generated by the model to the HIMU and extreme EMII compositions.

6. Acknowledgements

Rosemary Jones and Chris Ballentine acknowledge the support of the NERC Deep Mantle Volatiles consortium funding, NE/M000427/1. Peter van Keken and Jonathan Tucker acknowledge funding through the National Science Foundation CSEDI grant #1664642. We are grateful to Marianne Hasselhoff for assistance with Newton iteration coding. [We extend our thanks to Catherine Chauvel and an anonymous reviewer for their thorough and thoughtful comments, which have greatly improved the manuscript. Mike Bickle is thanked for editorial handling.](#)

7. Figure and table captions

Figure 1. ϵ_{Hf} and ϵ_{Nd} values for mid ocean ridge basalts (MORB) and ocean island basalts (OIB). The data were downloaded from the PetDB (www.earthchem.org/petdb) and GEOROC (<http://georoc.mpch-mainz.gwdg.de/georoc/>) databases in July 2017. The average compositions of the main mantle endmembers (DMM, FOZO, HIMU, EM) are shown by the large coloured squares,

where EMI and EMII are treated as a single endmember due to their similar compositions in these isotope systems. The data used to calculate the average compositions were filtered as follows. DMM: all MORB data; HIMU: all St. Helena data (type locality), high $^{206}\text{Pb}/^{204}\text{Pb}$ (>20.0), and low $^{87}\text{Sr}/^{86}\text{Sr}$ (<0.7036); EM: all Kerguelen and Society data (EMI and EMII type localities) and high $^{87}\text{Sr}/^{86}\text{Sr}$ (>0.7045); FOZO: high $^3\text{He}/^4\text{He}$ (where $R/R_a > 8$) and low $^{87}\text{Sr}/^{86}\text{Sr}$ (<0.704). The ϵ_{Hf} and ϵ_{Nd} compositions of the upper continental crust (not shown) are -13.2 ± 2.0 , and -10.3 ± 1.2 respectively (Chauvel et al., 2014)). The Hf-Nd mantle array follows the relationship $\epsilon_{\text{Hf}} = 1.44\epsilon_{\text{Nd}} + 1.61$; this is consistent with previously suggested relationships (e.g., Chauvel et al., 2008; Vervoort et al., 2011).

Figure 2. A schematic of the geodynamical-geochemical model. In order to save on computational time, the geochemical modelling is run as a post-processing step where we access the logged melting information for each of the tracers in the geodynamical model output and compute the model chemistry based on melting events, radioactive decay/radiogenic ingrowth with time, and extraction and recycling of the continental crust.

[Table 1. Published mineral/melt partition coefficients \(Kd\) and published/calculated bulk partition coefficients \(bulk D\) using different mineral modes. These are used and evaluated in the geodynamical-geochemical modelling.](#)

Table 2. Constant parameters in the geochemical model.

Figure 3. Plots of ϵ_{Nd} versus ϵ_{Hf} comparing the model chemistry (after 4.55 Byr with various bulk D values) to the global MORB-OIB dataset; a) bulk D values of Workman and Hart (2005); b) Kd values from Kelemen et al. (2003) combined with the mineral abundances for [DMM at 2 GPa](#) from Salters and Stracke (2004); c) bulk D values from Salters and Stracke (2004) for [DMM at 2 GPa \(i.e., without garnet\)](#); d) bulk D values from Salters and Stracke (2004) for [DMM at 3 GPa \(i.e., with garnet\)](#); e) bulk D values from Workman and Hart (2005) for Sm and Nd, and from Salters and Stracke (2004) for Lu and Hf ([DMM at 2 GPa](#)); and f) bulk D values from Workman and Hart (2005) for Sm and Nd, bulk D

value from Salters and Stracke (2004) for Lu ([DMM at 2 GPa](#)), and an assumed bulk D value of 0.066 for Hf. The formation of continental crust (CC) is not implemented in these models and all models use 10% excess eclogite density (EED=10%) as this always produces the most extreme range in values. Note the changing axis values and that the model data is coloured according to depth.

Figure 4. Plots of final ϵ_{Nd} versus ϵ_{Hf} (a, b, c) and average ϵ_{Hf} versus mantle depth as a function of model time (d, e, f) for different excess eclogite densities (EED); a and d show the results for the neutral case (EED=0%); b and e for 7% EED; and, c and f for 10% EED. These models assume the bulk D values from Workman and Hart (2005) for Sm and Nd, the bulk D value from Salters and Stracke (2004) for Lu ([DMM at 2 GPa](#)), and a bulk D value of 0.066 for Hf. No continental crust (CC) was produced in these models.

Figure 5. Plots of final ϵ_{Hf} compositions and ^{176}Hf concentrations (atoms/g) in the mantle after 4.55 Byr of mantle convection for different EED; a and d show the results for the neutral case (EED=0%); b and e for 7% EED; and, c and f for 10% EED. Plots of final ϵ_{Nd} compositions and ^{143}Nd concentrations (atoms/g) are shown in Supplementary Figure S1.

Figure 6. Plots of final ϵ_{Nd} versus ϵ_{Hf} (a and d), and the time evolution of average ϵ_{Hf} versus mantle depth (b and e) and the mass of the continental crust (in 10^{25} g; frames c and f). The top row shows the results for the model in which one present-day mass of the continental crust (CC_{pd}) is formed from 0.5 Byr. The bottom row shows the results for the model where continental crust was both generated and recycled from 0.5 Byr ($2\times\text{CC}_{pd}$ extracted, $1\times\text{CC}_{pd}$ recycled). Both models are for EED=10% using the preferred partition coefficients detailed in section 3.2. The results for EED=0% and EED=7% can be found in Supplementary Figures S2 and S3.

Table 3. Model results for different EED, BSE values, bulk D values, melt fractions, timing of crust production, and assumptions on production and recycling of continental crust. Here the upper mantle is considered to be at depths in the model of between 100 (i.e., below the melting zone) and

360 km. The Hf and Nd concentrations (ppm) of an upper mantle melt are calculated by applying batch melting equations to the average composition of the upper mantle, with varying melt fractions. These calculated concentrations are compared to those reported by Jenner and O'Neill (2012) for a MORB with 9 wt.% MgO (1.3 ppm Hf and 5.5 ppm Nd, Figure S4); the closest calculated values are underlined. The preferred model (Fig. 7) is highlighted in bold. An extended table is given in the Supplementary Data Tables.

Figure 7. Plots of final ϵ_{Nd} versus ϵ_{Hf} (a), average ϵ_{Hf} versus mantle depth (b), and average ϵ_{Nd} versus mantle depth (c) for the preferred model (EED=10%, continental crust produced and recycled, and bulk D values set to maximum values ($Sm=0.0670$, $Nd=0.0220$, $Lu=0.464$ and $Hf=0.075$) to achieve upper mantle ϵ_{Hf} and ϵ_{Nd} compositions and reasonable trace element compositions (Table 3)). Results without continental crust formation and recycling and 7% EED are shown in Figures S5 and S6.

Video. ϵ_{Hf} evolution of the mantle over 4.55 Byr of mantle convection, with 0.5 Byr time steps, for the preferred model (10% EED, continental crust produced and recycled, and bulk D values set to maximum values to achieve upper mantle ϵ_{Hf} and ϵ_{Nd} compositions and reasonable trace element compositions (see Table 3)).

8. References

- Albarède, F., 1998. Time-dependent models of U–Th–He and K–Ar evolution and the layering of mantle convection. *Chemical Geology*, 145, (3-4), p. 413-429.
- Allègre, C.J., Lewin, E., 1995. Isotopic systems and stirring times of the Earth's mantle. *Earth and Planetary Science Letters*, 136, (3-4), p. 629-646.
- Allègre, C.J., Rousseau, D., 1984. The growth of the continent through geological time studied by Nd isotope analysis of shales. *Earth and Planetary Science Letters*, 67, (1), p. 19-34.
- Aoki, I., Takahashi, E., 2004. Density of MORB eclogite in the upper mantle. *Physics of the Earth and Planetary Interiors*, 143-144, p. 129-143.
- Armstrong, R., 1981. Radiogenic isotopes: the case for crustal recycling on a near-steady-state no-continental-growth Earth. *Philosophical Transactions of the Royal Society of London A*, 301, (1461), p. 443-472.
- Belousova, E., Kostitsyn, Y., Griffin, W.L., Begg, G.C., O'Reilly, S.Y., Pearson, N.J., 2010. The growth of the continental crust: constraints from zircon Hf-isotope data. *Lithos*, 119, (3-4), p. 457-466.
- Bickle, M.J., 1986. Implications of melting for stabilisation of the lithosphere and heat loss in the Archaean. *Earth and Planetary Science Letters*, 80, (3), p. 314-324.

579 Bizimis, M., Griselein, M., Lassiter, J.C., Salters, V.J.M., Sen, G., 2007. Ancient recycled mantle
 580 lithosphere in the Hawaiian plume: Osmium–Hafnium isotopic evidence from peridotite mantle
 581 xenoliths. *Earth and Planetary Science Letters*, 257, (1), p. 259-273.
 582 Bouvier, A., Vervoort, J.D., Patchett, P.J., 2008. The Lu–Hf and Sm–Nd isotopic composition of CHUR:
 583 constraints from unequilibrated chondrites and implications for the bulk composition of terrestrial
 584 planets. *Earth and Planetary Science Letters*, 273, (1-2), p. 48-57.
 585 Bowring, S.A., Williams, I.S., 1999. Priscoan (4.00–4.03 Ga) orthogneisses from northwestern
 586 Canada. *Contributions to Mineralogy and Petrology*, 134, (1), p. 3-16.
 587 Brandenburg, J., Hauri, E.H., van Keken, P.E., Ballentine, C.J., 2008. A multiple-system study of the
 588 geochemical evolution of the mantle with force-balanced plates and thermochemical effects. *Earth
 589 and Planetary Science Letters*, 276, (1-2), p. 1-13.
 590 Brandenburg, J., van Keken, P., 2007. Deep storage of oceanic crust in a vigorously convecting
 591 mantle. *Journal of Geophysical Research*, 112, (B6), B06403.
 592 Chauvel, C., Blichert-Toft, J., 2001. A hafnium isotope and trace element perspective on melting of
 593 the depleted mantle. *Earth and Planetary Science Letters*, 190, (3), p. 137-151.
 594 Chauvel, C., Garçon, M., Bureau, S., Besnault, A., Jahn, B.-m., Ding, Z., 2014. Constraints from loess
 595 on the Hf–Nd isotopic composition of the upper continental crust. *Earth and Planetary Science
 596 Letters*, 388, p. 48-58.
 597 Chauvel, C., Hofmann, A.W., Vidal, P., 1992. HIMU-EM: The French Polynesian connection. *Earth and
 598 Planetary Science Letters*, 110, (1), p. 99-119.
 599 Chauvel, C., Lewin, E., Carpentier, M., Arndt, N.T., Marini, J.-C., 2008. Role of recycled oceanic basalt
 600 and sediment in generating the Hf–Nd mantle array. *Nature Geoscience*, 1, (1), p. 64-67.
 601 Christensen, U.R., Hofmann, A.W., 1994. Segregation of subducted oceanic crust in the convecting
 602 mantle. *Journal of Geophysical Research: Solid Earth*, 99, (B10), p. 19867-19884.
 603 Coltice, N., Ricard, Y., 1999. Geochemical observations and one layer mantle convection. *Earth and
 604 Planetary Science Letters*, 174, (1), p. 125-137.
 605 Condie, K.C., Aster, R.C., 2010. Episodic zircon age spectra of orogenic granitoids: the supercontinent
 606 connection and continental growth. *Precambrian Research*, 180, (3-4), p. 227-236.
 607 Condie, K.C., Bickford, M., Aster, R.C., Belousova, E., Scholl, D.W., 2011. Episodic zircon ages, Hf
 608 isotopic composition, and the preservation rate of continental crust. *Geological Society of America
 609 Bulletin*, 123, (5-6), p. 951-957.
 610 Davies, G.F., 2002. Stirring geochemistry in mantle convection models with stiff plates and slabs.
 611 *Geochimica et Cosmochimica Acta*, 66, (17), p. 3125-3142.
 612 Dhuime, B., Hawkesworth, C.J., Cawood, P.A., Storey, C.D., 2012. A change in the geodynamics of
 613 continental growth 3 billion years ago. *Science*, 335, (6074), p. 1334-1336.
 614 Eisele, J., Sharma, M., Galer, S.J.G., Blichert-Toft, J., Devey, C.W., Hofmann, A.W., 2002. The role of
 615 sediment recycling in EM-1 inferred from Os, Pb, Hf, Nd, Sr isotope and trace element systematics of
 616 the Pitcairn hotspot. *Earth and Planetary Science Letters*, 196, (3-4), p. 197-212.
 617 Elliott, T., Zindler, A., Bourdon, B., 1999. Exploring the kappa conundrum: the role of recycling in the
 618 lead isotope evolution of the mantle. *Earth and Planetary Science Letters*, 169, (1), p. 129-145.
 619 Fisher, C.M., Vervoort, J.D., 2018. Using the magmatic record to constrain the growth of continental
 620 crust—The Eoarchean zircon Hf record of Greenland. *Earth and Planetary Science Letters*, 488, p. 79-
 621 91.
 622 Fisher, C.M., Vervoort, J.D., DuFrane, S.A., 2014. Accurate Hf isotope determinations of complex
 623 zircons using the “laser ablation split stream” method. *Geochemistry, Geophysics, Geosystems*, 15,
 624 (1), p. 121-139.
 625 Gardiner, N.J., Johnson, T.E., Kirkland, C.L., Smithies, R.H., 2018. Melting controls on the lutetium–
 626 hafnium evolution of Archaean crust. *Precambrian Research*, 305, p. 479-488.
 627 Hanyu, T., Kawabata, H., Tatsumi, Y., Kimura, J.-I., Hyodo, H., Sato, K., Miyazaki, T., Chang, Q.,
 628 Hirahara, Y., Takahashi, T., Senda, R., Nakai, S.i., 2014. Isotope evolution in the HIMU reservoir

629 beneath St. Helena: Implications for the mantle recycling of U and Th. *Geochimica et Cosmochimica*
630 *Acta*, 143, p. 232-252.

631 Hawkesworth, C., Cawood, P.A., Dhuime, B., 2019. Rates of generation and growth of the continental
632 crust. *Geoscience Frontiers*, 10, (1), p. 165-173.

633 Hawkesworth, C.J., Kemp, A.I.S., 2006. Using hafnium and oxygen isotopes in zircons to unravel the
634 record of crustal evolution. *Chemical Geology*, 226, (3), p. 144-162.

635 Herzberg, C., Condie, K., Korenaga, J., 2010. Thermal history of the Earth and its petrological
636 expression. *Earth and Planetary Science Letters*, 292, (1), p. 79-88.

637 Hirose, K., Takafuji, N., Sata, N., Ohishi, Y., 2005. Phase transition and density of subducted MORB
638 crust in the lower mantle. *Earth and Planetary Science Letters*, 237, (1), p. 239-251.

639 Hirschmann, M.M., Stolper, E.M., 1996. A possible role for garnet pyroxenite in the origin of the
640 "garnet signature" in MORB. *Contributions to Mineralogy and Petrology*, 124, (2), p. 185-208.

641 Hofmann, A.W., 1988. Chemical differentiation of the Earth: the relationship between mantle,
642 continental crust, and oceanic crust. *Earth and Planetary Science Letters*, 90, (3), p. 297-314.

643 Hofmann, A.W., 1997. Mantle geochemistry: the message from oceanic volcanism. *Nature*, 385,
644 (6613), p. 219-229.

645 Irifune, T., 1987. An experimental investigation of the pyroxene-garnet transformation in a pyrolite
646 composition and its bearing on the constitution of the mantle. *Physics of the Earth and Planetary*
647 *Interiors*, 45, (4), p. 324-336.

648 Jacobsen, S.B., Wasserburg, G., 1979. The mean age of mantle and crustal reservoirs. *Journal of*
649 *Geophysical Research: Solid Earth*, 84, (B13), p. 7411-7427.

650 Jenner, F.E., O'Neill, H.S.C., 2012. Analysis of 60 elements in 616 ocean floor basaltic glasses.
651 *Geochemistry, Geophysics, Geosystems*, 13, (1), Q02005.

652 Johnson, T.E., Brown, M., Gardiner, N.J., Kirkland, C.L., Smithies, R.H., 2017. Earth's first stable
653 continents did not form by subduction. *Nature*, 543, p. 239-242.

654 Jones, R.E., Kirstein, L.A., Kasemann, S.A., Dhuime, B., Elliott, T., Litvak, V.D., Alonso, R., Hinton, R.,
655 2015. Geodynamic controls on the contamination of Cenozoic arc magmas in the southern Central
656 Andes: Insights from the O and Hf isotopic composition of zircon. *Geochimica et Cosmochimica Acta*,
657 164, p. 386-402.

658 Kelemen, P.B., Yogodzinski, G.M., Scholl, D.W., 2003. Along-strike variation in the Aleutian island arc:
659 Genesis of high Mg# andesite and implications for continental crust, In: Eiler, J. (Ed.), *Inside the*
660 *Subduction Factory*. American Geophysical Union, Washington DC, pp. 223-276.

661 Kellogg, J.B., Jacobsen, S.B., O'Connell, R.J., 2007. Modeling lead isotopic heterogeneity in mid-ocean
662 ridge basalts. *Earth and Planetary Science Letters*, 262, (3-4), p. 328-342.

663 Kessel, R., Schmidt, M.W., Ulmer, P., Pettke, T., 2005. Trace element signature of subduction-zone
664 fluids, melts and supercritical liquids at 120-180 km depth. *Nature*, 437, p. 724-727.

665 Kesson, S.E., Fitz Gerald, J.D., Shelley, J.M.G., 1994. Mineral chemistry and density of subducted
666 basaltic crust at lower-mantle pressures. *Nature*, 372, p. 767-769.

667 Kinny, P.D., Maas, R., 2003. Lu-Hf and Sm-Nd isotope systems in zircon. *Reviews in Mineralogy and*
668 *Geochemistry*, 53, (1), p. 327-341.

669 Kogiso, T., Tatsumi, Y., Nakano, S., 1997. Trace element transport during dehydration processes in
670 the subducted oceanic crust: 1. Experiments and implications for the origin of ocean island basalts.
671 *Earth and Planetary Science Letters*, 148, (1-2), p. 193-205.

672 Kumari, S., Paul, D., Stracke, A., 2016. Open system models of isotopic evolution in Earth's silicate
673 reservoirs: Implications for crustal growth and mantle heterogeneity. *Geochimica et Cosmochimica*
674 *Acta*, 195, p. 142-157.

675 Li, M., McNamara, A.K., Garnero, E.J., 2014. Chemical complexity of hotspots caused by cycling
676 oceanic crust through mantle reservoirs. *Nature Geoscience*, 7, p. 366-370.

677 Liu, C.-Z., Snow, J.E., Hellebrand, E., Brüggemann, G., von der Handt, A., Büchl, A., Hofmann, A.W.,
678 2008. Ancient, highly heterogeneous mantle beneath Gakkel ridge, Arctic Ocean. *Nature*, 452, p.
679 311-316.

680 McCulloch, M.T., Bennett, V.C., 1994. Progressive growth of the Earth's continental crust and
681 depleted mantle: Geochemical constraints. *Geochimica et Cosmochimica Acta*, 58, (21), p. 4717-
682 4738.

683 McDonough, W.F., Sun, S.-S., 1995. The composition of the Earth. *Chemical geology*, 120, (3-4), p.
684 223-253.

685 McKenzie, D., Bickle, M., 1988. The volume and composition of melt generated by extension of the
686 lithosphere. *Journal of petrology*, 29, (3), p. 625-679.

687 Ono, S., Ohishi, Y., Isshiki, M., Watanuki, T., 2005. In situ X-ray observations of phase assemblages in
688 peridotite and basalt compositions at lower mantle conditions: Implications for density of subducted
689 oceanic plate. *Journal of Geophysical Research: Solid Earth*, 110, (B2), B02208.

690 Palme, H., O'Neill, H.S.C., 2003. Cosmochemical Estimates of Mantle Composition, In: Carlson, R.W.
691 (Ed.), *The Mantle and Core, Volume 2*. In: Holland, H.D., Turekian, K.K. (Eds.), *Treatise on*
692 *Geochemistry*, 1, Elsevier, Oxford, pp. 1-38.

693 Peucker-Ehrenbrink, B., Hofmann, A.W., Hart, S.R., 1994. Hydrothermal lead transfer from mantle to
694 continental crust: the role of metalliferous sediments. *Earth and Planetary Science Letters*, 125, (1),
695 p. 129-142.

696 Ricolleau, A., Perrillat, J.P., Fiquet, G., Daniel, I., Matas, J., Addad, A., Menguy, N., Cardon, H.,
697 Mezouar, M., Guignot, N., 2010. Phase relations and equation of state of a natural MORB:
698 Implications for the density profile of subducted oceanic crust in the Earth's lower mantle. *Journal of*
699 *Geophysical Research: Solid Earth*, 115, (B8), B08202.

700 Ringwood, A.E., 1990. Slab-mantle interactions: 3. Petrogenesis of intraplate magmas and structure
701 of the upper mantle. *Chemical Geology*, 82, p. 187-207.

702 Ritsema, J., Deuss, A., Van Heijst, H., Woodhouse, J., 2011. S40RTS: a degree-40 shear-velocity model
703 for the mantle from new Rayleigh wave dispersion, teleseismic traveltimes and normal-mode splitting
704 function measurements. *Geophysical Journal International*, 184, (3), p. 1223-1236.

705 Rudge, J.F., McKenzie, D., Haynes, P.H., 2005. A theoretical approach to understanding the isotopic
706 heterogeneity of mid-ocean ridge basalt. *Geochimica et Cosmochimica Acta*, 69, (15), p. 3873-3887.

707 Rudnick, R., Gao, S., 2014. Composition of the Continental Crust, In: Rudnick, R. (Ed.), *The Crust*,
708 *Volume 4*. In: Holland, H.D., Turekian, K.K. (Eds.), *Treatise on Geochemistry*, 2, Elsevier, Amsterdam,
709 pp. 1-51.

710 Salters, V.J., Stracke, A., 2004. Composition of the Depleted Mantle. *Geochemistry, Geophysics,*
711 *Geosystems*, 5, (5), Q05B07.

712 Salters, V.J., White, W.M., 1998. Hf isotope constraints on mantle evolution. *Chemical Geology*, 145,
713 (3), p. 447-460.

714 Salters, V.J.M., Hart, S.R., 1989. The hafnium paradox and the role of garnet in the source of mid-
715 ocean-ridge basalts. *Nature*, 342, p. 420-422.

716 Sleep, N.H., Windley, B.F., 1982. Archean plate tectonics: constraints and inferences. *The Journal of*
717 *Geology*, 90, (4), p. 363-379.

718 Spasojevic, S., Gurnis, M., Sutherland, R., 2010. Mantle upwellings above slab graveyards linked to
719 the global geoid lows. *Nature Geoscience*, 3, (6), p. 435-438.

720 Stracke, A., Hofmann, A.W., Hart, S.R., 2005. FOZO, HIMU, and the rest of the mantle zoo.
721 *Geochemistry, Geophysics, Geosystems*, 6, (5), Q05007.

722 Stracke, A., Snow, J.E., Hellebrand, E., Von Der Handt, A., Bourdon, B., Birbaum, K., Günther, D.,
723 2011. Abyssal peridotite Hf isotopes identify extreme mantle depletion. *Earth and Planetary Science*
724 *Letters*, 308, (3), p. 359-368.

725 Tatsumoto, M., Basu, A.R., Wankang, H., Junwen, W., Guanghong, X., 1992. Sr, Nd, and Pb isotopes
726 of ultramafic xenoliths in volcanic rocks of Eastern China: enriched components EMI and EMII in
727 subcontinental lithosphere. *Earth and Planetary Science Letters*, 113, (1), p. 107-128.

728 Van der Hilst, R., Widiyantoro, S., Engdahl, E., 1997. Evidence for deep mantle circulation from global
729 tomography. *Nature*, 386, (6625), p. 578-584.

van Keken, P., 2001. Cylindrical scaling for dynamical cooling models of the Earth. *Physics of the Earth and Planetary Interiors*, 124, (1-2), p. 119-130.

van Keken, P., 2013. Mantle mixing: processes and modelling, In: Karato, S. (Ed.), *Physics and Chemistry of the Earth's Deep Interior*. John Wiley & Sons, Chichester, pp. 351-371.

Vervoort, J.D., Blichert-Toft, J., 1999. Evolution of the depleted mantle: Hf isotope evidence from juvenile rocks through time. *Geochimica et Cosmochimica Acta*, 63, (3), p. 533-556.

Vervoort, J.D., Kemp, A.I., 2016. Clarifying the zircon Hf isotope record of crust–mantle evolution. *Chemical Geology*, 425, p. 65-75.

Vervoort, J.D., Patchett, P.J., Blichert-Toft, J., Albarède, F., 1999. Relationships between Lu–Hf and Sm–Nd isotopic systems in the global sedimentary system. *Earth and Planetary Science Letters*, 168, (1), p. 79-99.

Vervoort, J.D., Plank, T., Prytulak, J., 2011. The Hf–Nd isotopic composition of marine sediments. *Geochimica et Cosmochimica Acta*, 75, (20), p. 5903-5926.

Weaver, B.L., 1991. The origin of ocean island basalt end-member compositions: trace element and isotopic constraints. *Earth and Planetary Science Letters*, 104, (2), p. 381-397.

White, W.M., 1985. Sources of oceanic basalts: Radiogenic isotopic evidence. *Geology*, 13, (2), p. 115-118.

White, W.M., 2015. Probing the Earth's deep interior through geochemistry. *Geochemical Perspectives*, 4, (2), p. 95-251.

White, W.M., Hofmann, A.W., 1982. Sr and Nd isotope geochemistry of oceanic basalts and mantle evolution. *Nature*, 296, p. 821–825.

Willbold, M., Stracke, A., 2006. Trace element composition of mantle end-members: Implications for recycling of oceanic and upper and lower continental crust. *Geochemistry, Geophysics, Geosystems*, 7, (4).

Willbold, M., Stracke, A., 2010. Formation of enriched mantle components by recycling of upper and lower continental crust. *Chemical Geology*, 276, (3), p. 188-197.

Workman, R.K., Hart, S.R., 2005. Major and trace element composition of the depleted MORB mantle (DMM). *Earth and Planetary Science Letters*, 231, (1), p. 53-72.

Xie, S., Tackley, P.J., 2004. Evolution of U-Pb and Sm-Nd systems in numerical models of mantle convection and plate tectonics. *Journal of Geophysical Research*, 109, (B11), B11204.

Zegers, T.E., van Keken, P.E., 2001. Middle Archean continent formation by crustal delamination. *Geology*, 29, (12), p. 1083-1086.

Zindler, A., Hart, S., 1986. Chemical geodynamics. *Review of Earth and Planetary Sciences*, 14, (1), p. 493-571.

Figure 1 low resolution
[Click here to download high resolution image](#)

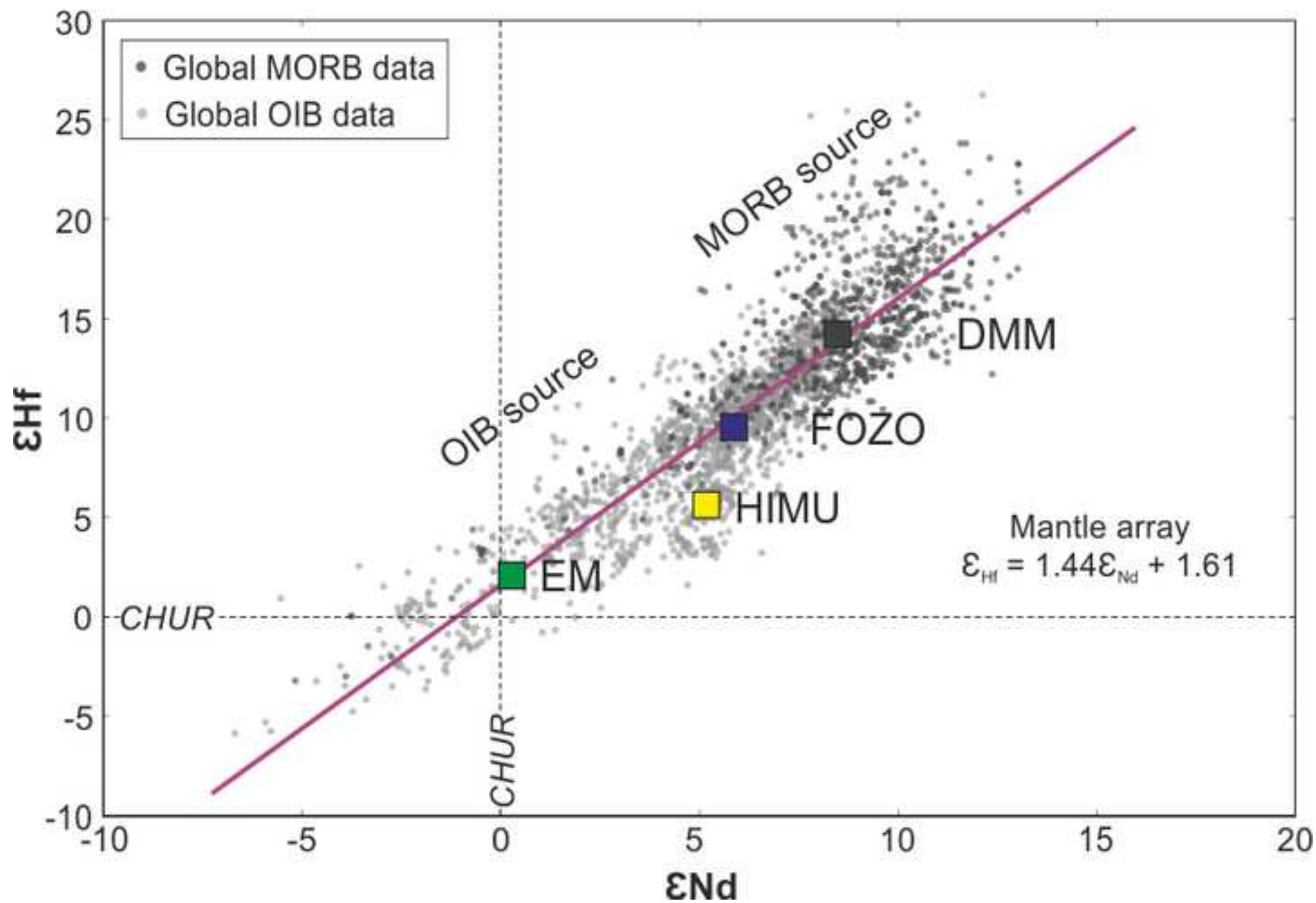


Figure 2 revised low resolution
[Click here to download high resolution image](#)

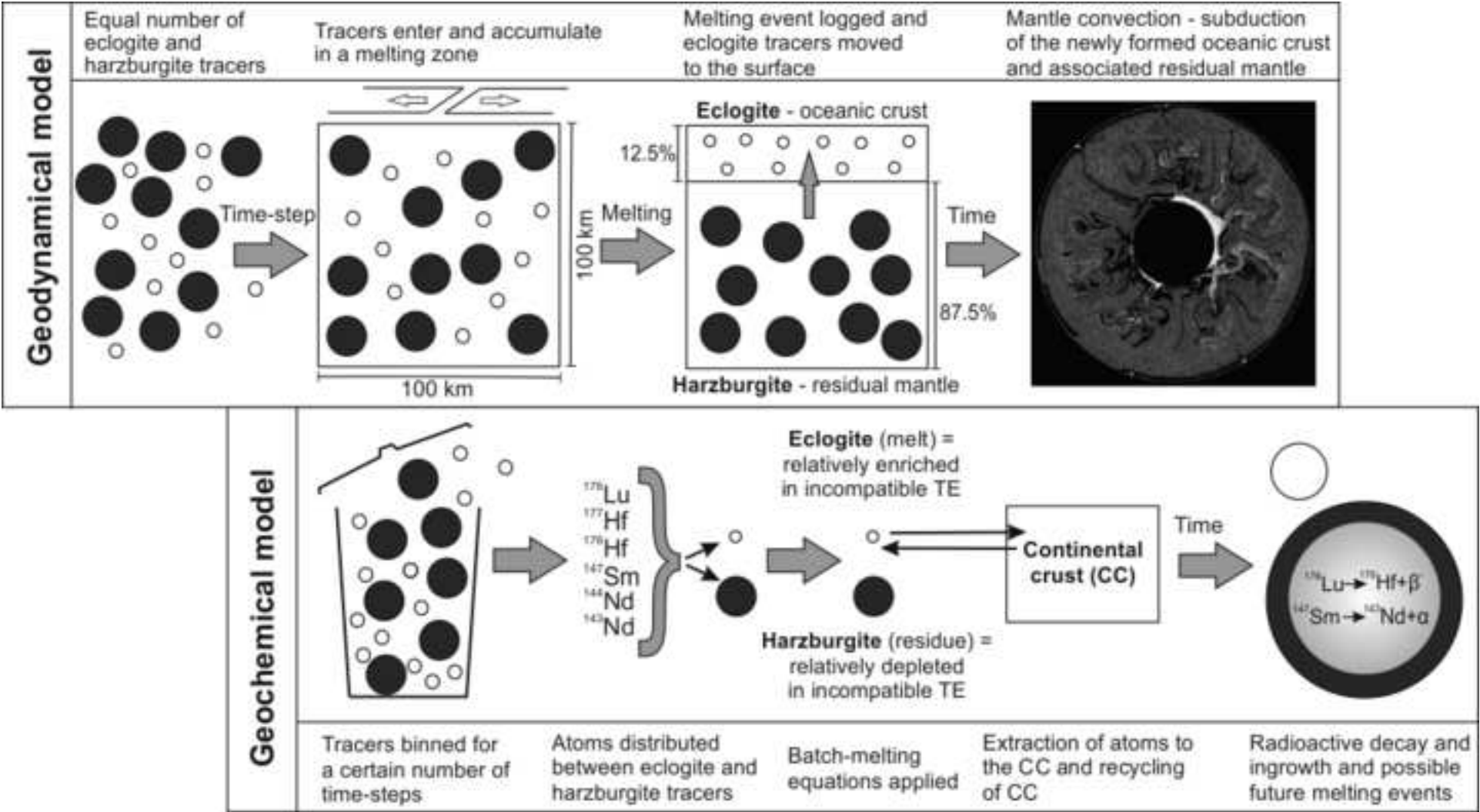


Figure 3 revised low resolution
[Click here to download high resolution image](#)

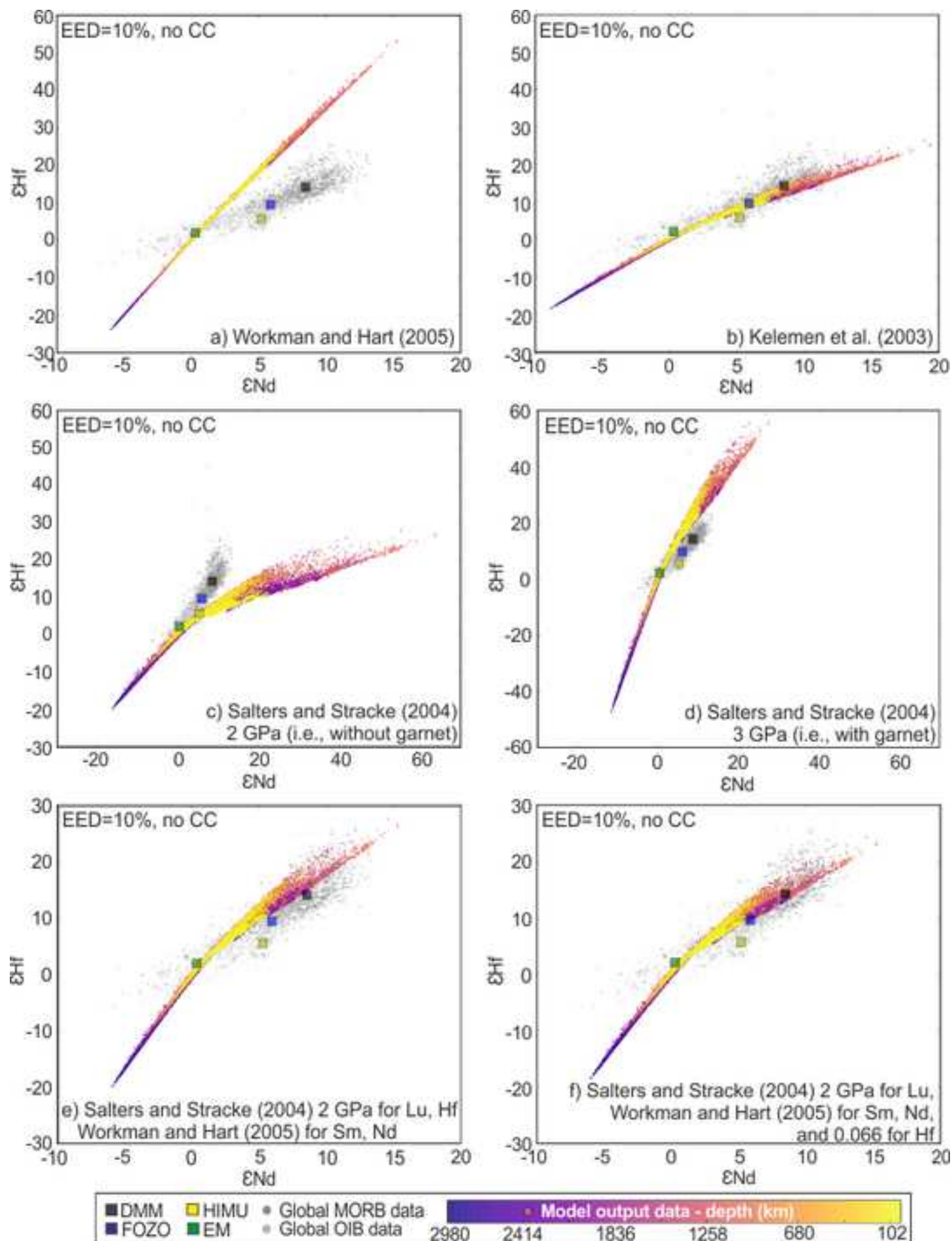


Figure 4 low resolution
[Click here to download high resolution image](#)

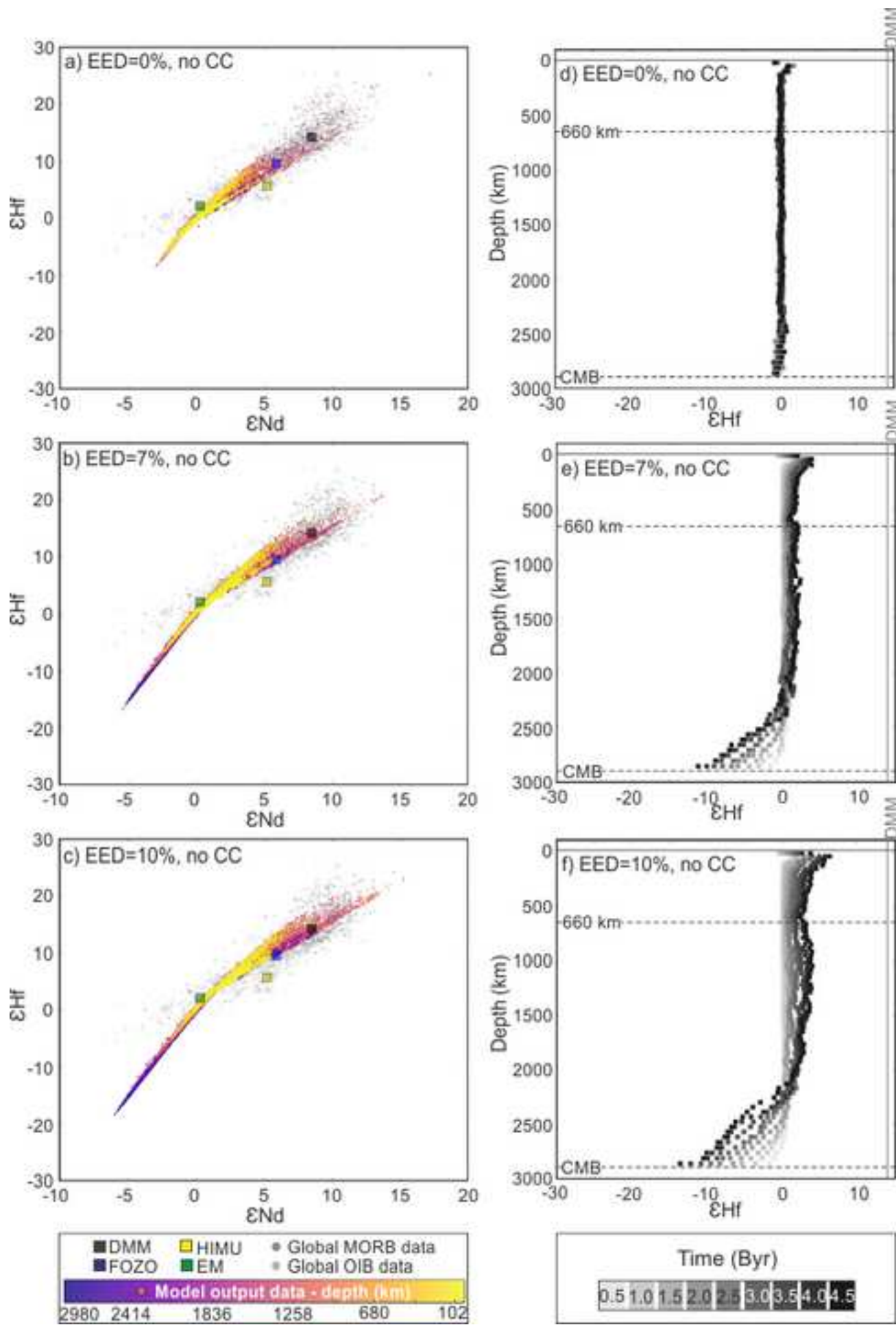


Figure 5 low resolution

[Click here to download high resolution image](#)

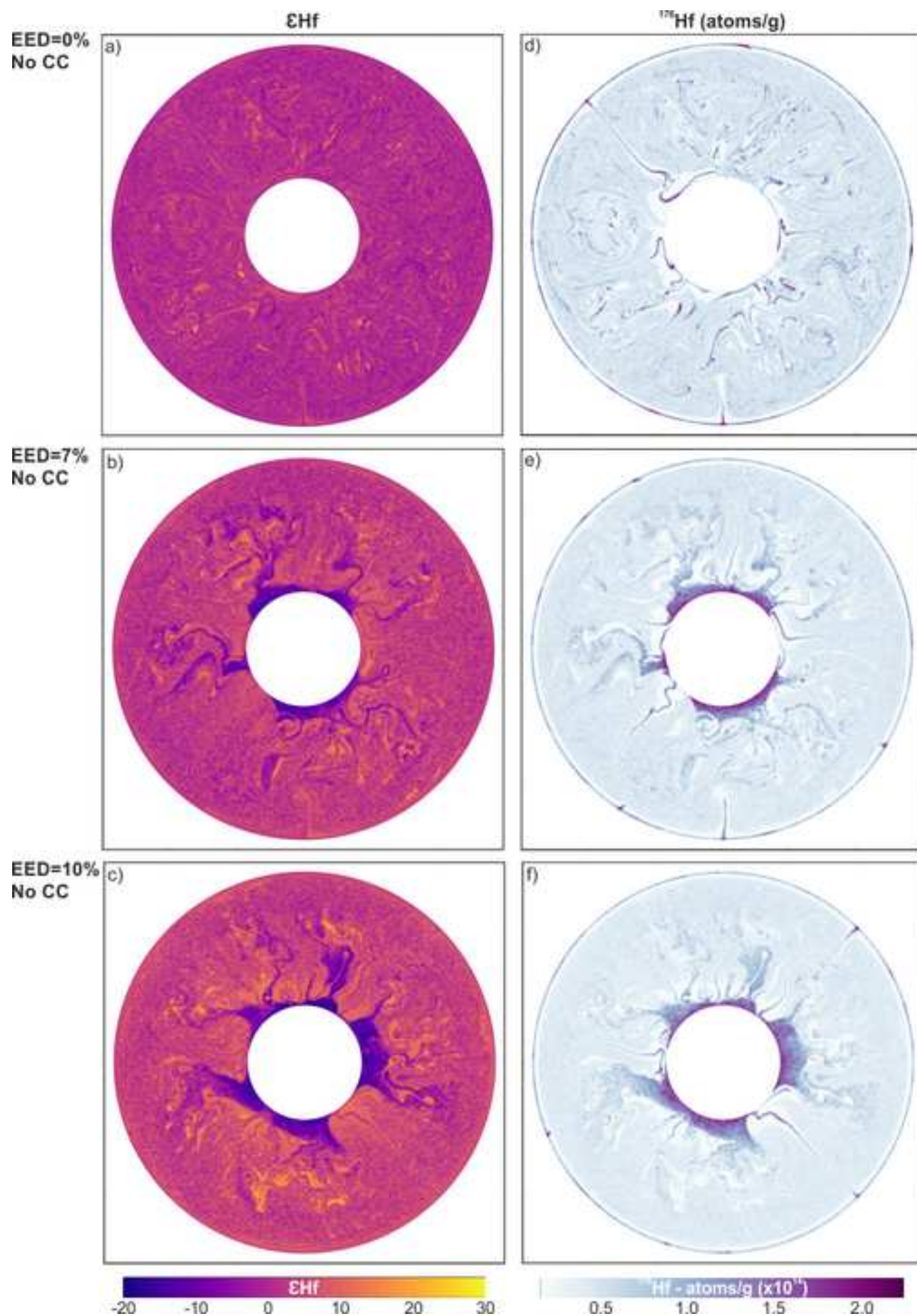


Figure 6 revised low resolution
[Click here to download high resolution image](#)

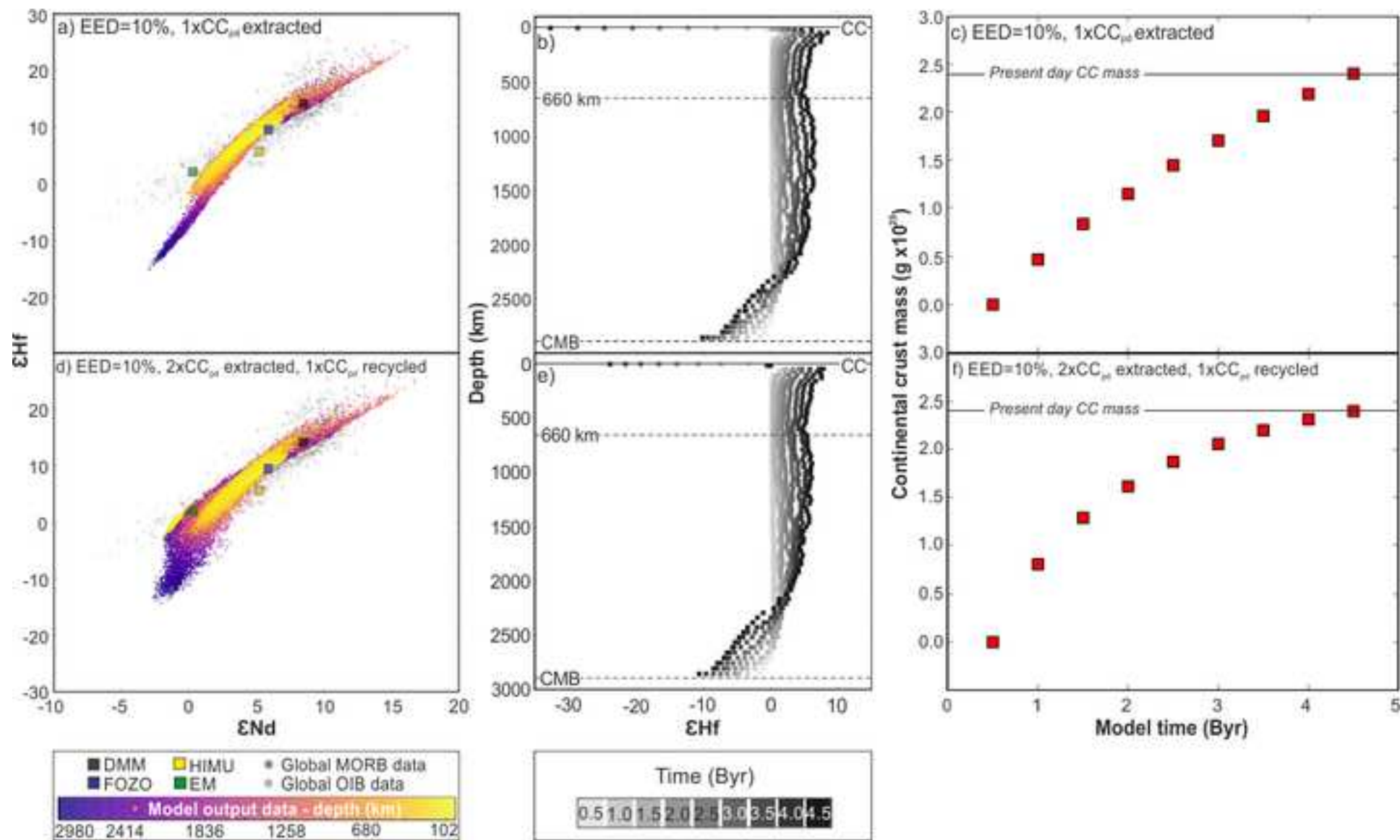


Figure 7 low resolution
[Click here to download high resolution image](#)

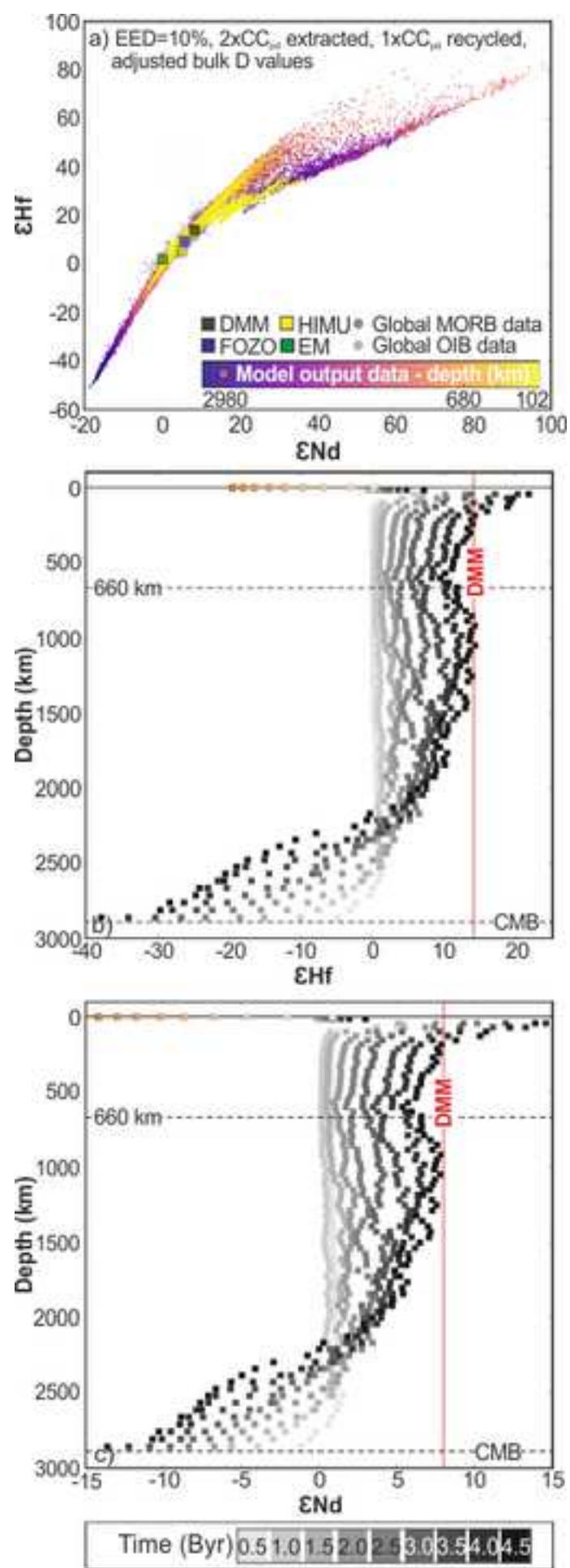


Table 1 revised
Click here to download Table: Table 1_revised.docx

Reference	Element	Mineral/melt partition coefficients (Kd)				Mineral mode (refer to table below)	Bulk D values				DSm/ DNd	DLu/ DHf	(DLu/DHf)/ (DSm/DNd)	Associated figure
		Olivine	Opx	Cpx	Garnet		Sm	Nd	Lu	Hf				
Workman and Hart (2005)	-	-	-	-	-	Depleted MORB mantle (DMM)	0.045	0.031	0.120	0.035	1.45	3.43	2.36	Fig. 3a
Salters and Stracke (2004) - 2 GPa	Sm	0.0011	0.02	0.299	-	Depleted MORB mantle (DMM)	0.045	0.015	0.111	0.047	3.00	2.40	0.80	
	Nd	0.00042	0.012	0.088	-	Salters and Stracke (2004) - 2 GPa - DMM	0.060	0.020	0.137	0.061	3.08	2.26	0.73	Fig. 3c
	Lu	0.02	0.12	0.511	-	Primitive mantle (PM)	0.065	0.021	0.141	0.065	3.16	2.18	0.69	
	Hf	0.0022	0.03	0.2835	-									
Salters and Stracke (2004) - 3 GPa	Sm	0.0011	0.02	0.1509	0.23	Salters and Stracke (2004) - 3 GPa - DMM	0.065	0.034	0.464	0.070	1.89	6.62	3.51	Fig. 3d
	Nd	0.00042	0.012	0.0884	0.064	PM including garnet	0.041	0.022	0.300	0.044	1.88	6.74	3.59	
	Lu	0.02	0.12	0.276	7									
	Hf	0.0011	0.024	0.14	0.4									
Kelemen et al. (2003)	Sm	0.0007	0.02	0.291	0.217	Depleted MORB mantle (DMM)	0.044	0.027	0.107	0.047	1.63	2.29	1.40	
	Nd	0.00007	0.009	0.1873	0.057	Primitive mantle (PM)	0.063	0.040	0.131	0.063	1.60	2.09	1.31	
	Lu	0.03	0.12	0.433	9	PM including garnet	0.067	0.039	0.395	0.075	1.69	5.30	3.13	
	Hf	0.004	0.04	0.256	0.5	Salters and Stracke (2004) - 2 GPa - DMM	0.059	0.036	0.129	0.060	1.61	2.15	1.34	Fig 3b
Average							0.055	0.028	0.204	0.057	2.098	3.545	1.886	
Max							0.067	0.040	0.464	0.075	3.157	6.743	3.587	
Min							0.041	0.015	0.107	0.035	1.452	2.095	0.690	

Mineral modes				
	Olivine	Opx	Cpx	Garnet
Depleted MORB mantle (DMM)	0.57	0.28	0.13	0
Salters and Stracke (2004) - 2 GPa - DMM	0.53	0.29	0.18	0
Salters and Stracke (2004) - 3 GPa - DMM	0.53	0.08	0.34	0.05
Primitive mantle (PM)	0.57	0.23	0.20	0
PM including garnet	0.56	0.22	0.19	0.03

Table 2
[Click here to download Table: Table 2.docx](#)

Fixed parameters			Reference
Age of the Earth (years)		4.55×10^9	
Mass of the mantle (g)		4.04×10^{27}	
Mass of the continental crust (g)		2.40×10^{25}	
Concentration of stable isotope species in the mantle (atoms/g)	^{144}Nd	1.242×10^{15}	Calculated using BSE values of McDonough and Sun (1995) and isotope abundances of Meija et al. (2016)
	^{177}Hf	1.776×10^{14}	
Decay constants (y^{-1})	^{147}Sm	6.53915×10^{-12}	Begemann et al. (2001)
	^{176}Lu	1.867×10^{-11}	Söderlund et al. (2004)
CHUR values	$^{147}\text{Sm}/^{144}\text{Nd}$	0.1960	Bouvier et al. (2008)
	$^{143}\text{Nd}/^{144}\text{Nd}$	0.512630	
	$^{176}\text{Lu}/^{177}\text{Hf}$	0.0336	
	$^{176}\text{Hf}/^{177}\text{Hf}$	0.282785	
Concentration of isotope species in the continental crust (atoms/g)	^{147}Sm	5.623×10^{40}	Calculated using continental crust composition of Rudnick and Gao (2014) and isotope abundances of Meija et al. (2016)
	^{144}Nd	4.769×10^{41}	
	^{176}Lu	6.441×10^{38}	
	^{177}Hf	5.573×10^{40}	

Table 3 revised
Click here to download Table: Table 3_revised.docx

Geochemical model inputs								Geochemical model outputs				Batch melting the upper mantle							Associated figure
EED model	Key parameter change	BSE values	Bulk D values				Continental crust	Average upper mantle		Element	Average upper mantle (ppm)	Varying melt fraction							
			Sm	Nd	Lu	Hf		Epsilon Hf	Epsilon Nd			0.01	0.05	0.1	0.125	0.15	0.2		
EED010	Adjusted bulk D values	McDonough and Sun (1995)	0.0450	0.0310	0.137	0.066	None	4.0	1.6	Hf Nd	0.23 0.97	3.09 23.95	2.07 12.26	<u>1.46</u> 7.62	<u>1.27</u> 6.41	1.13 <u>5.53</u>	0.92 <u>4.33</u>	Fig. 3f	
EED010	Adjusted bulk D values	McDonough and Sun (1995)	0.0670	0.0150	0.464	0.048	Production and recycling	14.4	8.0	Hf Nd	0.22 0.88	3.75 35.49	2.26 13.73	<u>1.51</u> 7.77	<u>1.29</u> <u>6.38</u>	1.13 <u>5.42</u>	0.91 <u>4.16</u>	Fig. 7	
EED010	No continental crust	McDonough and Sun (1995)	0.0670	0.0150	0.464	0.048	None	12.0	6.0	Hf Nd	0.23 0.94	3.95 37.89	2.38 14.66	1.59 8.30	<u>1.36</u> 6.82	<u>1.19</u> <u>5.79</u>	0.95 <u>4.44</u>	Fig. S5	
EED007	Lower EED (7%)	McDonough and Sun (1995)	0.0670	0.0150	0.464	0.048	Production and recycling	9.0	5.3	Hf Nd	0.23 0.95	3.95 38.09	2.38 14.73	1.59 8.34	<u>1.36</u> 6.85	<u>1.19</u> <u>5.82</u>	0.95 <u>4.47</u>	Fig. S6	
EED010	Late stage mantle depletion (after 0.75 Byrs)	McDonough and Sun (1995)	0.0670	0.0150	0.464	0.048	Production and recycling	10.6	6.3	Hf Nd	0.23 0.93	3.92 37.37	2.36 14.45	1.57 8.18	<u>1.35</u> 6.72	<u>1.18</u> <u>5.71</u>	0.94 <u>4.38</u>	Fig. S8	
EED010	Different BSE starting values	Palme and O'Neill (2003)	0.0670	0.0150	0.464	0.048	Production and recycling	14.2	7.8	Hf Nd	0.23 0.94	3.99 37.81	2.40 14.62	1.60 8.28	<u>1.37</u> 6.80	<u>1.20</u> <u>5.77</u>	0.96 <u>4.43</u>	-	
EED010	25% increase in melt fraction (F)	McDonough and Sun (1995)	0.0670	0.0150	0.464	0.048	Production and recycling	14.5	7.1	Hf Nd	0.21 0.87	3.69 35.19	2.22 13.61	<u>1.48</u> 7.70	<u>1.27</u> <u>6.33</u>	1.11 <u>5.37</u>	0.89 4.12	Fig. S9	

Figure S1

[Click here to download Supplementary material for online publication only: Figure S1.tif](#)

Figure S2 revised

[Click here to download Supplementary material for online publication only: Figure S2_revised.tif](#)

Figure S3 revised

[Click here to download Supplementary material for online publication only: Figure S3_revised.tif](#)

Figure S4

[Click here to download Supplementary material for online publication only: Figure S4.tif](#)

Figure S5

[Click here to download Supplementary material for online publication only: Figure S5.tif](#)

Figure S6

[Click here to download Supplementary material for online publication only: Figure S6.tif](#)

Figure S7

[Click here to download Supplementary material for online publication only: Figure S7.tif](#)

Figure S8

[Click here to download Supplementary material for online publication only: Figure S8.tif](#)

Figure S9 new

[Click here to download Supplementary material for online publication only: Figure S9.tif](#)

Supplementary material - extended methods and figures

[Click here to download Supplementary material for online publication only: Supplementary Information_revised.docx](#)

Supplementary Data Tables_revised

[Click here to download Supplementary material for online publication only: Supplementary Data Tables_revised.xlsx](#)

Supplementary material (video) - Epsilon Hf evolution

[Click here to download Supplementary material \(video\): Epsilon Hf evolution over 4.55Byr for preferred model EED010.mp4](#)